

# Isoprene NO<sub>3</sub> Oxidation Products from the RO<sub>2</sub> + HO<sub>2</sub> Pathway

## Supplemental Information

*Rebecca H. Schwantes<sup>†\*</sup>, Alexander P. Teng<sup>†</sup>, Tran B. Nguyen<sup>†</sup>, Matthew M. Coggon<sup>‡</sup>, John D. Crounse<sup>†</sup>, Jason M. St. Clair<sup>#⊥</sup>, Xuan Zhang<sup>†</sup>, Katherine A. Schilling<sup>‡</sup>, John H. Seinfeld<sup>‡§</sup>, Paul O. Wennberg<sup>†§</sup>*

<sup>†</sup>Division of Geological and Planetary Sciences, California Institute of Technology, 1200 E.  
California Blvd, Pasadena, CA 91125

<sup>‡</sup>Division of Chemistry and Chemical Engineering, California Institute of Technology, 1200 E.  
California Blvd, Pasadena, CA 91125

<sup>§</sup>Division of Engineering and Applied Science, California Institute of Technology, 1200 E.  
California Blvd, Pasadena, CA 91125

<sup>#</sup>Atmospheric Chemistry and Dynamics Laboratory, NASA Goddard Space Flight Center,  
Greenbelt, MD, USA

<sup>⊥</sup>Joint Center for Earth Systems Technology, University of Maryland Baltimore County,  
Baltimore, MD, USA

\*Corresponding author. E-mail: rschwant@caltech.edu, or Paul Wennberg  
(wennberg@gps.caltech.edu)

## **S1.0 KINETIC MECHANISM DEVELOPMENT.**

A kinetic mechanism is formulated to simulate the reaction conditions of these experiments. The reactions included are listed in the Appendix (Table SA2, SA3, and SA4). Table SA5 contains a list of the abbreviations used. Rate constants for most of the reactions included in the mechanism are based on recommendations from JPL<sup>1</sup>, IUPAC<sup>2-3</sup>, or MCM v3.2<sup>4</sup>. However, some rate constants and branching ratios are not known. For these, we use our best judgement based on available data; explanations of the assumptions on which these estimates are based are included in this section. Some branching ratios and rate constants are estimated based on the experimental results presented here. Many of these branching ratios depend on the fraction of  $\delta$ - and  $\beta$ -isomers that form (Table 3 and 5), which will likely depend on the lifetime of the RO<sub>2</sub> radical (Section 4.1). Thus, the reaction products and rates presented here are most consistent with the experimental results for this study in which the overall RO<sub>2</sub> lifetime was  $\sim 30$  s. The kinetic mechanism developed here represents our current level of understanding, and deviations from the experimental results highlight areas for future study.

**S1.1. Basic Reactions in Kinetic Mechanism.** HO<sub>2</sub> was constrained in the kinetic mechanism by the measured H<sub>2</sub>O<sub>2</sub> production rate. Prior to photooxidation, H<sub>2</sub>O<sub>2</sub> is predominantly formed from HO<sub>2</sub> + HO<sub>2</sub> reactions. To match the observed H<sub>2</sub>O<sub>2</sub> production rate in experiments 5, 6, and 8, we arbitrarily increased the reaction rate constant for CH<sub>2</sub>O + NO<sub>3</sub> by a factor of 2.5-3 in the kinetic mechanism above that recommended by IUPAC. Although not perfect when correcting for the missing HO<sub>2</sub> in this manner, the H<sub>2</sub>O<sub>2</sub> curves for the kinetic mechanism and the experimental results were fairly consistent. Under-prediction of HO<sub>2</sub> could be caused by other

missing chemistry including unaccounted for surface chemistry, later generation chemistry not incorporated into the kinetic mechanism, or many other possibilities. Here, we are confident that there is a missing source of  $\text{HO}_2$ , but are agnostic about the mechanism responsible.

Because the predominant loss of isoprene is due to reaction with  $\text{NO}_3$ , the measured isoprene decay rate was used to constrain the amount of  $\text{NO}_3$  present. Cantrell et al.<sup>5</sup> proposed that  $\text{N}_2\text{O}_5$  would react with water present on the wall surface to form nitric acid even under dry conditions. We included a wall loss rate for  $\text{N}_2\text{O}_5$  (i.e.,  $\text{NO}_3$  loss rate) such that the isoprene decay in the kinetic mechanism matched with experimental results. This rate constant is chamber/experiment specific. For experiment 5 ( $24 \text{ m}^3$ , 2.2 ppm  $\text{CH}_2\text{O}$ ), 6 ( $24 \text{ m}^3$ , 4.7 ppm  $\text{CH}_2\text{O}$ ), 7 ( $1 \text{ m}^3$ , 2 ppm  $\text{CH}_2\text{O}$ ) and 8 ( $1 \text{ m}^3$ , 4 ppm  $\text{CH}_2\text{O}$ ),  $\text{N}_2\text{O}_5$  wall loss rate constants that best fit experimental conditions were  $1.5 \times 10^{-4}$ ,  $12 \times 10^{-4}$ ,  $6 \times 10^{-4}$  and  $12 \times 10^{-4} \text{ s}^{-1}$ , respectively. We observe that the  $\text{N}_2\text{O}_5$  loss rate appears to be sensitive to both the mixing ratio of  $\text{CH}_2\text{O}$  and the chamber. However, it should be noted that in calculating these  $\text{N}_2\text{O}_5$  wall loss rate constants,  $\text{N}_2\text{O}_5$  wall loss is assumed to be the only missing sink of  $\text{NO}_3$ . Possibly there are other unknown  $\text{NO}_3$  sinks as well, and this will impact the relative differences between the wall loss rate constants calculated above.

For experiment 10, methyl nitrite, isoprene,  $\text{NO}_2$ , and  $\text{H}_2\text{O}_2$  were injected into the chamber, and photooxidation was initiated. Isoprene reacted with  $\text{OH}$ , and  $\text{HO}_2$  was generated. The formation rate of  $\text{HO}_2$  was adjusted in the kinetic mechanism so that the ratio of isoprene hydroxy hydroperoxide (ISOPOOH) to isoprene hydroxy nitrate matched experimental results.  $\text{N}_2\text{O}_5$  loss to the walls was not needed in the kinetic mechanism for this experiment consistent with the hypothesis that the  $\text{N}_2\text{O}_5$  loss in the other experiments was enhanced by the presence of  $\text{CH}_2\text{O}$ .

**S1.2 First-Generation Chemistry.** The isoprene related reactions included in the kinetic mechanism are listed in Table SA3. The  $\text{RO}_2 + \text{RO}_2$  proposed reaction rates and  $\text{RO}_2 + \text{HO}_2$  proposed products are addressed in Sections 4.2 and 4.3. Not all isomers are included separately in the kinetic mechanism:  $\beta$ - and  $\delta$ -isomers are grouped together using the results from Tables 3 and 5. The generalized reaction rate constant determined in Section 4.2 is used in the kinetic mechanism for  $\text{INO}_2 + \text{INO}_2$ . The ToF-CIMS has been directly calibrated using IHN standards,<sup>6</sup> so the sensitivity for IHN is well constrained. When the maximum branching ratio reported by Kwan et al.<sup>7</sup> for the  $\text{R}'\text{CHO} + \text{ROH}$  pathway (0.77), the median value for the ROOR pathway (0.035), and the remainder for the 2RO pathway (0.195) are used in the kinetic mechanism, experimental and predicted results for IHN agree well (Figure 2). All further oxidized isoprene nitrooxyperoxy radicals are assumed to react at the same rate and product distribution as  $\text{INO}_2 + \text{INO}_2$ . For  $\text{INO}_2$  reactions with other  $\text{RO}_2$  species, the reaction rate constants are estimated by taking the geometric mean of the respective self-reaction rate constants. The products formed are assumed to be the same as the self-reactions (see Table SA3). This is clearly an approximation, but the exact product distributions are unknown.

In Section 4.2, we discussed that uncertainty in hydroxy methy peroxy (HMP) formation and reaction could influence the  $\text{C}_5$  nitrooxy peroxy ( $\text{INO}_2$ ) +  $\text{INO}_2$  reaction rate constants estimated by this study. To test this, we alter the following in the kinetic mechanism: use the  $\text{HMP} + \text{CH}_2\text{O}$  equilibrium rate constant measured by Zabel et al.<sup>8</sup> and increase the  $\text{HMP} + \text{HMP}$  reaction rate constant to the acetyl peroxy radical self-reaction rate constant ( $1.6 \times 10^{-11} \text{ cm}^3 \text{ molec}^{-1} \text{ s}^{-1}$ )<sup>2</sup>. Now the  $\text{INO}_2 + \text{INO}_2$  rate constant that best fits the data is  $\sim 3.5 \times 10^{-12} \text{ cm}^3 \text{ molec}^{-1} \text{ s}^{-1}$ . Formic acid is greatly under-predicted by the kinetic mechanism without these changes ( $\sim 95\%$  missing prior to photooxidation and  $\sim 85\%$  3.5 h after photooxidation). With these adjustments, predicted

formic acid is more consistent with experimental results (~ 50% missing prior to photooxidation and ~ 20% 3.5 h after photooxidation) although there are still significant differences. The magnitude of formic acid produced (~10 times the amount of isoprene reacted) is so large that it is highly likely a by-product of CH<sub>2</sub>O chemistry. We also test whether uncertainty in the H<sub>2</sub>O<sub>2</sub> concentration affects the estimation of  $k_{\text{INO}_2 + \text{INO}_2}$ . Even if H<sub>2</sub>O<sub>2</sub> were 20% lower, the kinetic mechanism still predicts  $k_{\text{INO}_2 + \text{INO}_2}$  to be  $\sim 4 \times 10^{-12} \text{ cm}^3 \text{ molec}^{-1} \text{ s}^{-1}$ .

**S1.3 Second-Generation Chemistry Rate Constants.** Lee et al.<sup>6</sup> determined the OH addition rate constants for  $\delta$ -[1,4N]-IHN (average between *cis*- and *trans*-) and  $\beta$ -[4,3N]-IHN to be  $1.1 \times 10^{-10}$  and  $4.2 \times 10^{-11} \text{ cm}^3 \text{ molec}^{-1} \text{ s}^{-1}$ , respectively. Because no other studies have directly measured OH rate constants for isoprene nitrates,  $k_{\text{OH}} = 1.1 \times 10^{-10} \text{ cm}^3 \text{ molec}^{-1} \text{ s}^{-1}$  is used for  $\delta$ -INP,  $\delta$ -IHN, and ICN and  $k_{\text{OH}} = 4.2 \times 10^{-11} \text{ cm}^3 \text{ molec}^{-1} \text{ s}^{-1}$  is used for  $\beta$ -[1,2]-INP,  $\beta$ -[4,3]-INP, and  $\beta$ -IHN. St. Clair et al.<sup>9</sup> determined that OH abstracts a hydrogen from the hydroperoxide group of [1,2]-ISOPOOH and [4,3]-ISOPOOH with the following rate constants,  $9.0 \times 10^{-12}$  and  $4.7 \times 10^{-12} \text{ cm}^3 \text{ molec}^{-1} \text{ s}^{-1}$ , respectively. For lack of more information, it is assumed that both the  $\beta$ - and  $\delta$ -INP undergo hydrogen abstraction from the hydroperoxide group at the average of these two rate constants. The hydrogen  $\alpha$  to the carbonyl group on ICN is also extractable. A rate constant ( $1.7 \times 10^{-11} \text{ cm}^3 \text{ molec}^{-1} \text{ s}^{-1}$ ) based on the SAR method<sup>10</sup> is used in the kinetic mechanism. The hydrogen abstraction rate is ~15% of the expected OH addition rate.

The O<sub>3</sub> addition rate constant for  $\delta$ -[1,4]-IHN (average between *cis*- and *trans*-) and  $\beta$ -[4,3]-IHN was measured by Lee et al.<sup>6</sup> to be  $2.8 \times 10^{-17}$  and  $2.6\text{--}5 \times 10^{-19} \text{ cm}^3 \text{ molec}^{-1} \text{ s}^{-1}$ , respectively. Lockwood et al.<sup>11</sup> measured the O<sub>3</sub> addition rate constant for  $\delta$ -[1,4]-*trans*-IHN,  $\beta$ -[1,2]-IHN, and  $\beta$ -[2,1]-IHN to be  $5.3 \times 10^{-17}$ ,  $1.06 \times 10^{-16}$ , and  $3.4 \times 10^{-16} \text{ cm}^3 \text{ molec}^{-1} \text{ s}^{-1}$ , respectively. The values measured by Lockwood et al.<sup>11</sup> are too fast to be consistent with the observed loss rate of IHN

during the nighttime at SOAS, so the rate constants measured by Lee et al. are incorporated into the kinetic mechanism, but this is an area for future research given the discrepancy between these two studies.  $k_{O_3}$  for  $\delta$ -IHN was assigned the value of  $2.8 \times 10^{-17} \text{ cm}^3 \text{ molec}^{-1} \text{ s}^{-1}$ , and  $k_{O_3}$  for  $\beta$ -[1,2]-INP,  $\beta$ -[4,3]-INP, and  $\beta$ -IHN is assigned to  $3.8 \times 10^{-19} \text{ cm}^3 \text{ molec}^{-1} \text{ s}^{-1}$ .

After most of the  $O_3$  had reacted away in experiment 6 (measured  $O_3 < 16$  ppb and modeled  $NO_3 < 6$  ppt), the stability of the main isoprene nitrates was monitored over 3.5 h to assess wall loss under the conditions of this study. The wall loss for INP, IHN, and ICN was measured to be  $9 \times 10^{-6}$ ,  $7 \times 10^{-6}$ , and  $6 \times 10^{-6} \text{ s}^{-1}$ , respectively. These wall loss rates are similar to the wall loss rates measured under different conditions for compounds of similar structure in the same chamber ( $24 \text{ m}^3$ )<sup>12</sup> and in the  $1 \text{ m}^3$  chamber<sup>6</sup>. These wall loss rates were incorporated into the kinetic mechanism.

Also in experiment 6, sequential amounts of  $O_3$  were added to the chamber to monitor the formation of later generation chemistry. The last  $O_3$  injection occurred after all isoprene had reacted. There was little loss of ICN, while IHN decayed the most. The nitrates were lost in many different ways (e.g., reaction with  $O_3$ , reaction with  $NO_3$ , and wall loss). The distribution of these losses is likely specific to the nitrate compound and isomer. Exact decay rates cannot be inferred from the kinetic mechanism because there are too many possible avenues. However, because ICN and INP decay slower than IHN, general  $O_3$  and  $NO_3$  rate constants were estimated based on the relative decay in experiment 6. The great differences in the decay curves alone suggest that  $O_3$  and/or  $NO_3$  reaction rates with ICN, INP, and IHN vary substantially. The relative  $O_3$  and  $NO_3$  reaction rate constants for ICN, INP, and IHN are assumed to be consistent. Rate constants for ICN and  $\delta$ -INP reaction with  $O_3$  were approximated by using the measured  $k_{O_3}$  for  $\delta$ -IHN<sup>6</sup> and the ratio of the lifetimes determined from the decay curve in experiment 6

corrected for the wall loss rates.  $k_{O_3}$  for ICN is an upper bound as  $m/z = (-) 248$  (INP) fragments in the Triple-CIMS to form products at  $m/z = (-) 230$  (same  $m/z$  as ICN) (See Section S3.0).

For  $NO_3$ , Rollins et al.<sup>13</sup> measured a combined isoprene nitrate rate constant of  $7 \times 10^{-14} \text{ cm}^3 \text{ molec}^{-1} \text{ s}^{-1}$  by fitting parameters to match experimental results in a kinetic mechanism largely based on MCM v3.1. This combined rate constant was based on total alkyl nitrate measurements made by Thermal Dissociation-Laser Induced Fluorescence and a variety of instruments that measured  $NO_3$  and  $N_2O_5$ . Incorporation of this rate constant for IHN, ICN, and INP into the kinetic mechanism produced a rate of decay of the products that exceeded the experimental results. Thus,  $k_{NO_3+IHN}$  is assumed to be  $7 \times 10^{-14} \text{ cm}^3 \text{ molec}^{-1} \text{ s}^{-1}$  and  $k_{NO_3+ICN}$  is estimated ( $8.1 \times 10^{-15} \text{ cm}^3 \text{ molec}^{-1} \text{ s}^{-1}$ ) based on the ratio of lifetimes in experiment 6 with a correction for wall loss. A lower reaction rate constant for ICN is expected. Other studies have measured low reaction rate constants for reaction of  $NO_3$  with unsaturated aldehydes (e.g.,  $k_{NO_3 + trans\text{-}2\text{-hexenal}} = 4.7 \times 10^{-15} \text{ cm}^3 \text{ molec}^{-1} \text{ s}^{-1}$ )<sup>14</sup>. The influence of a hydroperoxy group on  $NO_3$  reaction rate constants is unknown. The approach used to estimate  $k_{NO_3+ICN}$  over-estimated  $k_{NO_3+INP}$ , so a different approach was used based on the formation of isoprene dinitrooxyepoxide (IDNE), which Kwan et al.<sup>7</sup> proposed formed with a yield of 0.35. This yield is consistent with this study as well. IDNE forms from  $NO_3$  adding to the least substituted carbon of  $\beta$ -[1,2]-INP and  $\delta$ -[4,1]-INP, which make up 0.37 of all INP (Table 3). Predicted IDNE matches experimentally detected IDNE for experiment 5 (more  $NO_3$  oxidation of INP occurs in this experiment than experiment 8) when  $k_{NO_3+INP}$  is  $5 \times 10^{-15} \text{ cm}^3 \text{ molec}^{-1} \text{ s}^{-1}$ . This rate constant is substantially lower than that Rollins et al. predicted for the general rate constant. In the current system, IDNE could have a higher wall loss rate due to more nitric acid present in the chamber, which would cause  $k_{NO_3+INP}$  to be under-predicted.

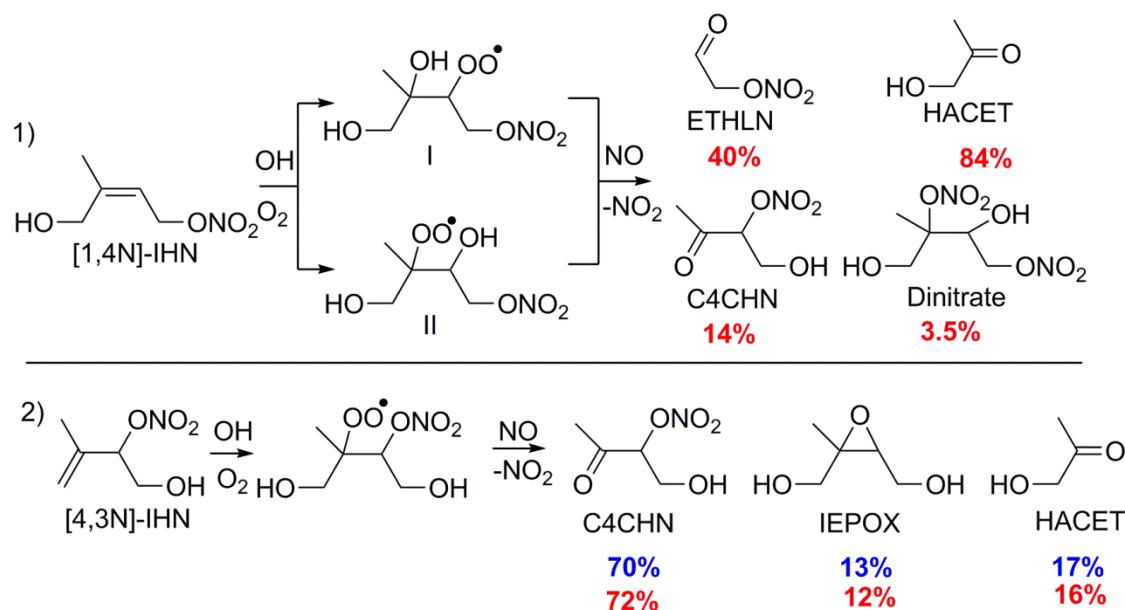
The rate constants of NO<sub>3</sub> with isoprene derived nitrates require further study with synthetic standards. Understanding the NO<sub>3</sub> reaction rate constants for the main nitrates from NO<sub>3</sub> oxidation is important, as without this knowledge models will not accurately depict which and how many of the nitrates survive through the night to react with OH at sunrise.

**S1.4 Second Generation Chemistry Product Distribution.** Product distributions and rate constants were incorporated based on the isomer distribution determined in this study (Table 3) and current literature understanding, but the kinetic mechanism was not further optimized. Given the complexity and the large number of unknowns, optimizing the kinetic mechanism for later-generation products has too many degrees of freedom. Standards for all of the primary products will need to be synthesized to understand fully the later generation chemistry.

Lee et al.<sup>6</sup> and Jacobs et al.<sup>15</sup> have both studied the products from the oxidation of isoprene hydroxy nitrates shown in Scheme S1. From the limited sample size available, it appears that the subsequent fragmentation following oxidation of the hydroxy nitrate is less likely to break the carbon bond next to a nitrate group than the carbon bond next to an OH group. Since all of the nitrates produced from NO<sub>3</sub> oxidation will contain a nitrate group on either the C<sub>1</sub> or C<sub>4</sub> carbon, the products formed are assumed to be similar to the distribution of products from [1,4N]-IHN. Lee et al.<sup>6</sup> did not detect a C<sub>4</sub> product without a nitrate group, so if there was a nitrate group  $\alpha$  to the peroxy group, it was assumed no C<sub>4</sub> products formed. Additionally, all the C<sub>4</sub> product detected by Lee et al.<sup>6</sup> from [1,4N]-IHN + OH was assumed to come from the second peroxy radical (Scheme S1).



**Scheme S1.** Isoprene nitrates reaction products that have been studied by Lee et al.<sup>6</sup> with adjusted HACET and IEPOX yields<sup>16</sup> in red and Jacobs et al.<sup>15</sup> in blue.



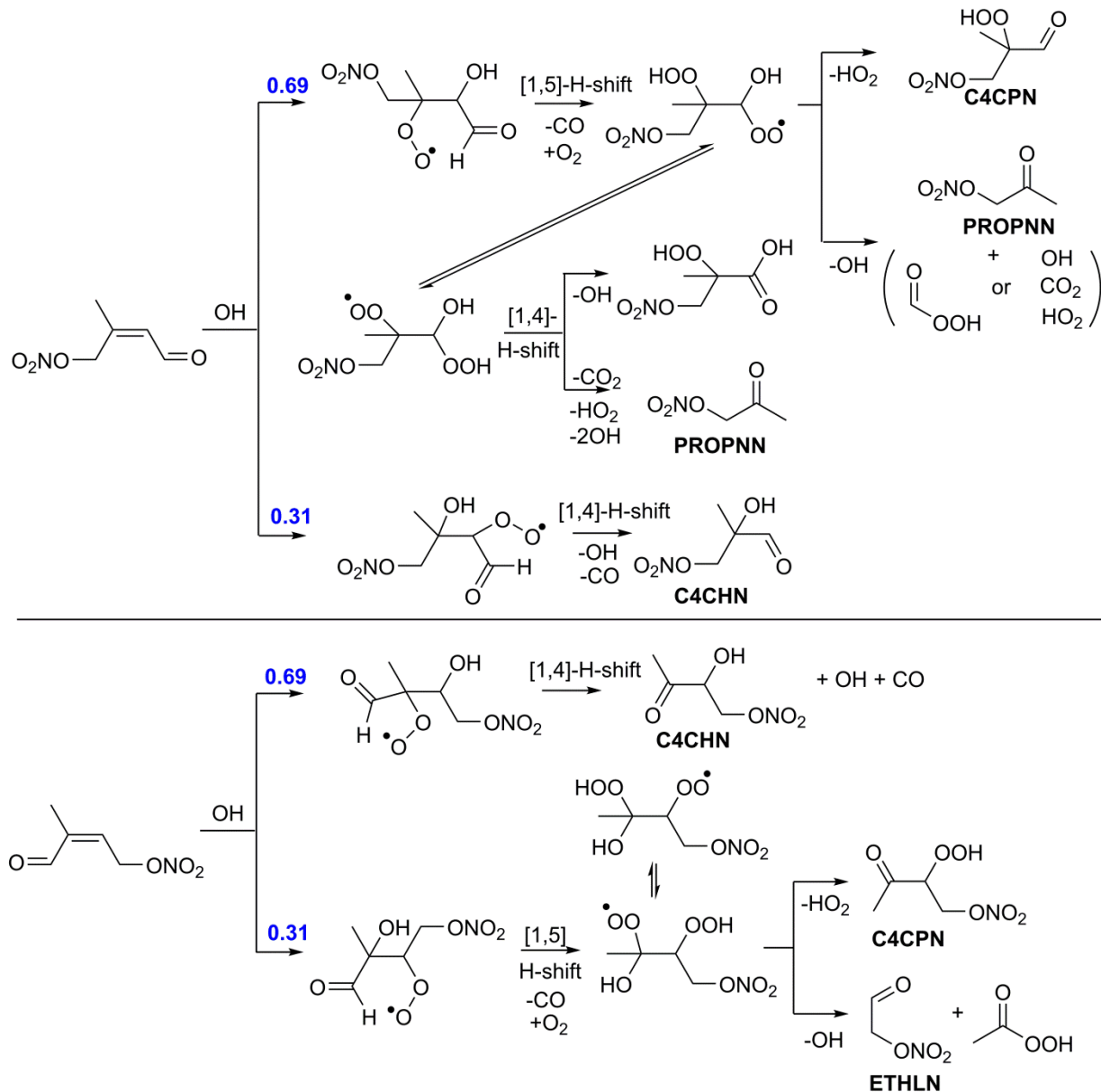
OH was assumed to add to the less substituted carbon. The branching ratios were determined based on compounds with a similar carbon backbone. Teng et al.<sup>17</sup> determined that OH added to the least substituted carbon 69% of the time for 2-methyl-2-butene, which has the same carbon backbone as the  $\delta$ -nitrates. For  $\beta$ -[1,2]-nitrates and  $\beta$ -[4,3]-nitrates, OH is assumed to add to the least substituted carbon similar to MVK<sup>18</sup> (76%) and MACR<sup>19</sup> (96.5%), respectively. An epoxide, like IEPOX, is assumed to form only if there is a nitrate group available to form an epoxide, otherwise the epoxide yield is distributed by weight to the other products. For INP, if OH adds in a position such that formation of an epoxide is possible, INHE is assumed to form in 100% yield (See Section 4.4.1 of the main work). Lee et al.<sup>6</sup> had NO levels higher than the atmosphere and the present study, which led to an unequal yield of hydroxyacetone (HACET) and ethanal nitrate (ETHLN). In this study (and in the atmosphere), these yields should be equivalent; 3.5% of dinitrates are assumed to form from NO reacting with any of the peroxy radicals formed from ICN, IHN, or INP.<sup>6</sup> Using results from Lee et al.<sup>6</sup> with revised HACET and

IEPOX yields,<sup>16</sup> 27% of hydroperoxides are assumed to form from HO<sub>2</sub> reacting with all peroxy radicals formed from the isoprene nitrates. Results from Table 3 with the assumptions stated above are used to predict the distribution of products for the  $\beta$ - and  $\delta$ -isomers of IHN, ICN, and INP (see Table SA3).

Figure 4 illustrates that with the above assumptions the kinetic mechanism over-predicts ETHLN to a small degree, and under-predicts C4CHN by a large fraction. It is possible that the carbonyl is a better leaving group than the hydroxy. In the kinetic mechanism, if we assume that when OH reacts with ICN, the bond next to the carbonyl group fragments forming C4CHN and CO (rather than breaking the bond connecting C<sub>2</sub> and C<sub>3</sub> of isoprene), the simulated C4CHN is increased and ETHLN is reduced. However, C4CHN is still under-predicted by the kinetic mechanism, suggesting that there is another reason for C4CHN under-prediction.

Several studies have determined that hydrogen shifts can occur fast enough to be relevant in the atmosphere.<sup>19-21</sup> Most chamber studies run at low RO<sub>2</sub> lifetimes do not detect this chemistry, even though this pathway is likely to be important in the atmosphere. In this study, when photooxidation was initiated, the kinetic mechanism estimates an overall RO<sub>2</sub> lifetime of ~0.4 s and ~1 s for experiments 5 and 8, respectively. These lifetimes are fairly short, but when OH reacts with ICN, likely both the [1,4]- and [1,5]-H-shifts are competitive (Scheme S2), as Crounse et al.<sup>19</sup> inferred a rate constant of 0.5 s<sup>-1</sup> for a similar [1,4]-H-shift for MACR, and the [1,5]-H-shift should be even faster.

**Scheme S2.** Possible H-shifts from OH oxidation of ICN.



The rate constants for peroxy radical shifts will depend on many factors, including neighboring substituents, degree of substitution, and type of hydrogen shift. Currently, a comparison of all of these factors has not been well constrained for peroxy radical shifts, but the influence of all of these factors has been summarized by Carter and Atkinson<sup>22</sup> for alkoxy radical shifts. In order to estimate the relevance of peroxy radical shifts in these experiments, the *relative* rate constant

differences for the degree of substitution and type of hydrogen shift is assumed to be similar for alkoxy and peroxy radicals. For example, if the [1,4]-H shift for ICN oxidation by OH is assumed to be similar to that of MVK ( $\sim 0.5 \text{ s}^{-1}$ ),<sup>19</sup> then the [1,5]-H shifts will occur at  $\sim 2 \times 10^3 \text{ s}^{-1}$  if peroxy and alkoxy radicals act similarly. Since the [1,5]-H shift occurs so quickly, reaction with NO/NO<sub>3</sub>/HO<sub>2</sub> is not incorporated as an option for this peroxy radical. Because the [1,4]-H shift is slower, both the possibility of a shift and reaction with NO/NO<sub>3</sub>/HO<sub>2</sub> are included in the kinetic mechanism. In the atmosphere both the [1,4]- and the [1,5]-H-shifts are expected to be important.

Given that a hydrogen  $\alpha$  to a nitrate group is  $\sim 200$  times less abstractable according to the SAR method<sup>10</sup>, shifts are not considered for this hydrogen. H-shifts for peroxy radicals with an  $\alpha$ -hydroxy/hydroperoxy group will be much slower than those with an  $\alpha$ -carbonyl group. For example, Crounse et al.<sup>21</sup> determined a minimum rate constant of  $0.1 \text{ s}^{-1}$  for a secondary [1,5]-H shift from a carbon containing a hydroperoxy group. Since primary hydrogen shifts occur slower than secondary hydrogen shifts for alkoxy radicals<sup>22</sup> and this effect is likely similar for peroxy radicals, H-shifts for peroxy radicals with an  $\alpha$ -hydroxy/hydroperoxy group are assumed not to occur under the conditions of the current study. These hydrogen shifts are still likely relevant in the atmosphere and deserve further attention, but the conditions in the current study are not optimal for identifying them.

The products from the O<sub>3</sub> oxidation of ICN, IHN, and INP are more complicated to predict based on currently available data than those from OH oxidation. The products from  $\beta$ -IHN or  $\beta$ -INP + O<sub>3</sub> were not included as  $k_{\text{O}_3}$  for  $\beta$ -isomers is expected to be quite low.

The product yields from 2-methyl-2-butene have been quantified by many studies. The C<sub>3</sub> and C<sub>2</sub> Criegee distribution is  $\sim 0.3$  and  $\sim 0.7$ <sup>23-24</sup>, respectively, and the OH yield is  $0.88$ <sup>2</sup>. Lee et al.

<sup>6</sup>, the only current study to measure how O<sub>3</sub> product yields are affected by nitrate or hydroxy groups, found *trans*-[1,4N]-IHN and *cis*-[1,4N]-IHN produced much less OH (0.2 and 0.48, respectively) than 2-methyl-2-butene. With the corrected HACET yields<sup>16</sup>, ETHLN and HACET yields were 0.50 and 0.48 for *trans*-[1,4N]-IHN and 0.55 and 0.93 for *cis*-[1,4N]-IHN, respectively. The non-unity yield of the carbonyl species suggests that something quenches the Criegee for the *cis*-isomer. Possibly acetone was interfering, as between 0.5-2 ppm of acetone was present and acetone reacts with formaldehyde oxide with a rate constant of  $2.3 \times 10^{-13} \text{ cm}^3 \text{ molec}^{-1} \text{ s}^{-1}$  (or  $\tau_{\text{acetone}} = 0.1\text{-}0.4 \text{ s}$ ).<sup>25</sup> Since we are unsure why a non-unity yield of carbonyl species formed for the *cis*-isomer, all nitrates in this work are assumed to react like *trans*-[1,4N]-IHN.

The concentrations of CO, NO (during photooxidation), and NO<sub>2</sub> were sufficient to quickly react with all of the Criegees that form. The O<sub>3</sub> reactions that have been included in the kinetic mechanism are based on the following assumptions: (1) all of the nitrates react with O<sub>3</sub> to form an equal number of C<sub>2</sub> and C<sub>3</sub> Criegees, (2) all C<sub>2</sub> Criegees are stabilized by CO, NO, or NO<sub>2</sub>, and (3) all C<sub>3</sub> Criegees form 0.4 OH and the rest is stabilized by CO, NO, or NO<sub>2</sub>.

A full set of products for the reaction of IHN, INP and ICN with NO<sub>3</sub> is not estimated in the kinetic mechanism as there are no direct studies of these reactions. In total, the kinetic mechanism predicts that 0.05 ppb of these second generation NO<sub>3</sub> products form for experiments 8, so this simplification is not expected to influence the decomposition product results. IDNE and OH are included with a yield of 0.35 as products for  $\delta$  and  $\beta$ -INP + NO<sub>3</sub> reactions.<sup>7</sup> Additionally, an epoxide could form from NO<sub>3</sub> adding to the least substituted carbon of [1,4]-IHN, -INP, and -ICN with release of a nitrate group (similar to OH addition to IHN to form IEPOX<sup>15</sup>). This is incorporated into the kinetic mechanism with a product yield of 0.13<sup>15</sup> for the isomer that will

produce an epoxide (e.g., 0.11 for all  $\delta$ -INP using the distribution in Table 3). The exact epoxide yield from isoprene nitrates reaction with  $\text{NO}_3$  should be measured, as studies have found that organic nitrate SOA growth at night forms largely from multigenerational chemistry.<sup>26</sup>

The rate constants and products of INHE + OH were predicted based on two IEPOX + OH product studies.<sup>27-28</sup> Jacobs et al.<sup>28</sup> measured much higher rate constants ( $\delta$ 4-IEPOX:  $3.52 \times 10^{-11}$ ,  $\beta$ -IEPOX:  $3.6 \times 10^{-11}$ ) then Bates et al.<sup>27</sup> ( $\delta$ 1-IEPOX:  $8.4 \times 10^{-12}$ , *cis*- $\beta$ -IEPOX  $1.52 \times 10^{-11}$ , *trans*- $\beta$ -IEPOX:  $9.8 \times 10^{-12}$ ). The reaction rate constants measured by Bates et al.<sup>27</sup> are used in the kinetic mechanism for  $\delta$ -INHE and  $\beta$ -INHE (average of the *trans* and *cis*). The products included in the kinetic mechanism for INHE reacting with OH are based on the products formed from OH reacting with  $\beta$ -IEPOX<sup>27</sup> and  $\delta$ 4-IEPOX<sup>28</sup>. The hydrogen  $\alpha$  to a nitrate group is assumed not to be abstractable, and the distribution of the INHE isomers was determined from results in Table 3 assuming OH adds to INP in the ratios described above.

**S1.5 Photolysis.** The photolysis reactions included in the kinetic mechanism are outlined in Table SA4. Most are based on recommendations from JPL<sup>1</sup> or MCM v3.2<sup>4</sup>. ISOPROOH and INP were assumed to photolyze at the same rate as methyl hydroperoxide like MCM v3.2<sup>4</sup> suggests. Preliminary evidence from a side experiment suggests that the photolysis rate for INP is much faster than the rate for methyl hydroperoxide. The absorption spectrum and quantum yields for INP deserve further attention as photolysis could be a competitive sink for INP in the atmosphere.

## **S2.0 PEAK ASSIGNMENTS FOR GC-ToF-CIMS.**

Because peak shapes were not perfect Gaussians, when compounds eluted fully separated from other isomers or when peak separation was not necessary, the area under the peak was determined by adding up all data points and multiplying by the sampling frequency. With co-

eluting isomers, peaks were fit assuming an exponentially broadened Gaussian peak shape. The time constant, peak position, width, and height were selected based on minimization of the root mean square fitting error. In all cases, the distribution of isomers was determined by the areas measured for the first GC run in any given experiment to avoid the influence of second generation chemistry and wall loss. Peak percentages determined by subsequent GC results were within 7%, 4%, and 12% of the first GC results for INP, ICN, and IHN, respectively.

Several of the GC-ToF-CIMS chromatographs for IHN during experiment 8 are shown in Figure S1. Synthesized standards were available for all of the IHN compounds formed in this work except [4N,3]-IHN.<sup>6,29</sup> Given the elution times of compounds with similar structures, we expect [4N,3]-IHN to elute right after [1N,2]-IHN, so we assign [4N,3]-IHN to peak 1.

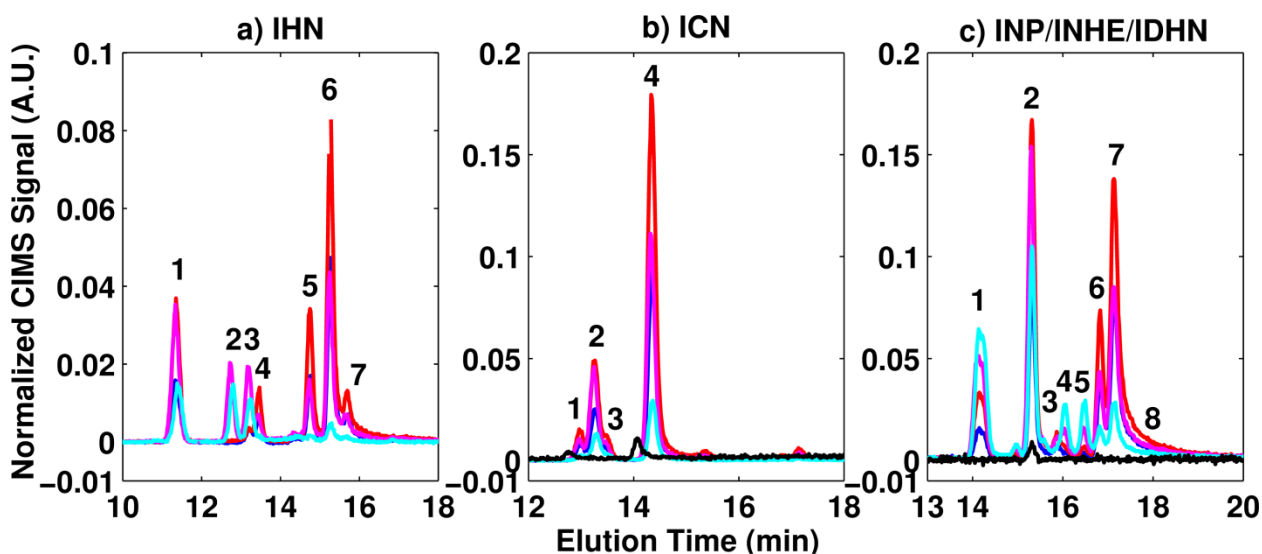


**Figure S1.** GC-ToF-CIMS chromatographs for experiment 8 as a function of time following the initiation of the photochemistry: -2.7h (blue), -0.6h (red), +0.9h (magenta), +2.9h (cyan), for panel b, 2 x  $m/z$  = (-)185 at +2.9h (black) and for panel c, 2 x  $m/z$  = (-)63 at -2.7h (black). See Table S1 for a list of isomers assigned to each peak.

**Table S1.** List of isomers assigned to each peak labeled in Figure S1.

peak #	1	2	3	4	5	6	7	8
a) IHN	[4N,3]	[1,2N]	[4,3N]	un-known	<i>cis</i> -[1N,4]	<i>trans</i> -[1N,4]- & <i>cis</i> -[4N,1]	<i>trans</i> -[4N,1]	NA
b) ICN	<i>cis</i> - $\delta$ -[4,1]	<i>trans</i> - $\delta$ -[4,1]	<i>cis</i> - $\delta$ -[1,4]	<i>trans</i> - $\delta$ -[1,4]	NA	NA	NA	NA
c) INP/INHE	$\delta$ -INHE & IDHN	$\beta$ -[1,2]-INP	$\beta$ -[4,3]-INP	<i>cis/trans</i> - $\beta$ -[4,1]-INHE		<i>cis</i> -[1,4]	<i>trans</i> -[1,4]- & <i>cis</i> -[4,1]	<i>trans</i> -[4,1]

The *trans*-[1N,4]-IHN and *cis*-[4N,1]-IHN isomers co-elute and so differentiating between these isomers is not possible. The distribution of the areas for peaks 5, 6, and 7 at 49 minutes after the start of NO<sub>3</sub> oxidation are 22%, 67%, and 11%, respectively. If there exists an equal amount of *cis*- and *trans*-isomers, the area under peaks 5 and 7 should equal the area under peak 6. This is clearly not the case, suggesting that either the *cis* and *trans* INO<sub>2</sub> species are not present in equal amounts or the RO<sub>2</sub> + RO<sub>2</sub> rates are quite different for the *cis* and *trans* peroxy radicals. Since the INO<sub>2</sub> distribution favors C<sub>1</sub> addition and the relative rates of  $\delta$ -[1,4]-INO<sub>2</sub> and  $\delta$ -[4,1]-INO<sub>2</sub> with RO<sub>2</sub> are expected to be similar to what Jenkin et al.<sup>30</sup> predicted, the *trans*-INO<sub>2</sub> fraction or *trans*-INO<sub>2</sub> + RO<sub>2</sub> rate constant must be ~3 times larger than those of the *cis*-isomer. Assuming that C<sub>1</sub> and C<sub>4</sub> addition products have the same ratio of *cis*- and *trans*-products, [4N,1]-IHN and [1N,4]-IHN make up 86% and 14% of  $\delta$ -IHN, respectively.

Several GC-ToF-CIMS chromatographs for ICN (m/z = (-) 230) are shown in Figure S1b. The only possible  $\beta$ -ICN is  $\beta$ -[4,3]-ICN. The  $\beta$ -[4N,3]-IHN standard elutes at least 3 min prior to any of the  $\delta$ -IHN isomers (Figure S1a) and isoprene hydroxy carbonyl species, which are both  $\delta$ -isomers (m/z = (-) 185), elute at nearly the same time as ICN, which suggests that none of the peaks at m/z = (-) 230 are  $\beta$ -ICN. The distribution of areas for peaks 1, 2, 3, and 4 at 49 minutes into photooxidation are 6%, 20%, 5%, and 69%, respectively. Because peak 4 represents most of



the signal, and many studies have already determined that C<sub>1</sub> addition is favored over C<sub>4</sub> addition,<sup>31-33</sup> we assign peak 4 to be either *trans*- and/or *cis*-[1,4]-ICN. This demonstrates that ICN behaves differently on the GC column than IHN (Table S1). Based on peak area we suspect peak 1 is *cis*-[4,1]-ICN and peak 2 is *trans*-[4,1]-ICN. We tentatively assign peak 3 to *cis*-[1,4]-ICN, but it is also quite possible that *cis*-[1,4]-ICN co-elutes with *trans*-[1,4]-ICN (peak 4). With these assumptions, 74% is [1,4]-ICN and 26% is [4,1]-ICN. These results compare well with a previous report, based predominantly on the isomer distribution of ICN,<sup>31</sup> that estimated C<sub>1</sub> addition (78%) to be favored over C<sub>4</sub> addition (22%). Because ICN peak assignments are largely based on area and other studies suggesting C<sub>1</sub> addition occurs more favorably than C<sub>4</sub> addition, the isomer distribution determined is more speculative than IHN and INP.

The chromatographs for m/z = (-) 248 (representing INP, C<sub>5</sub> dihydroxy nitrate (IDHN), and C<sub>5</sub> nitrooxy hydroxyepoxide (INHE)) are shown in Figure S1c. The combined presence of INHE, IDHN, and INP adds uncertainty in peak assignment. In addition, the GC transmission for m/z = (-) 248 through the 4 m column was only ~80% before the initiation of photooxidation unlike IHN and ICN, which was ~100%.  $\delta$ -INP in all chromatographs formed a large right-handed tail which adds uncertainty to peak fitting even assuming an exponentially broadened Gaussian peak shape. Because of this, GC results for experiment 10 (first GC, ~40 min into NO<sub>3</sub> oxidation) were used to determine the isomer distribution of INP. In this experiment, a shorter column (1m) and lower sample loading decreased the tailing and increased the transmission (~100%). Additionally, the influence of RO<sub>2</sub> + RO<sub>2</sub> chemistry on INP formation was lower in experiment 10 compared to the other experiments (see Section 3.0). Prior to the start of photooxidation the  $\beta$ - and  $\delta$ -isomer fractions were similar in experiment 7 (0.35 & 0.65), 8 (0.30 & 0.70 -assuming some loss of the  $\delta$ -isomers), and 10 (0.30 & 0.70). The  $\beta$ -isomers might be more favored in

experiment 7 due to differential isomer loss to the walls or reaction with  $O_3/NO_3$  because the first GC-ToF-CIMS was taken nearly 5 h after the start of  $NO_3$  oxidation.

Based on  $\beta$ -ISOPOOH standards<sup>27</sup> and the known ratio of  $C_1$  to  $C_4$  addition ( $\sim 3.5$ -  $7.4$ )<sup>31-32</sup> we suspect  $\beta$ -[1,2]-INP and  $\beta$ -[4,3]-INP to be peaks 2 and 3, respectively. The ratio of peak 2 to peak 3 decreases, in experiments 7, 8, and 10, as the influence of  $RO_2 + RO_2$  chemistry declines. This is consistent with the peak assignment order, since  $\beta$ -[4,3]-INO<sub>2</sub> is expected to have the highest  $RO_2$  rate constant of all the isomers (Section 4.2). Additionally, using MS/MS with the GC-Triple-CIMS we observe the (-) 63 product ion characteristic of hydroperoxide fragments<sup>34</sup> for both  $\beta$ -INP (peaks 2 and 3). In fact, even the  $\delta$ -INP (peaks 6-8) forms a small amount of the (-) 63 daughter, but the fraction is much lower than for  $\beta$ -INP.

We suspect that  $\delta$ -INP has the same elution order as  $\delta$ -IHN (Table S1). The distribution of areas for peaks 6, 7, and 8 at 40 min into photooxidation in experiment 10 is 31%, 59%, and 10% respectively. Similar to IHN, assuming  $C_1$  and  $C_4$  addition products produce the same ratio of *cis*- and *trans*-products, *trans* is favored 1.7 times over *cis*, and [1,4]-INP and [4,1]-INP make up 84% and 16% of  $\delta$ -INP.

Peaks 1, 4, and 5 in Figure S1c are assigned to INHE isomers. Based on the elution time of  $\delta$ - and  $\beta$ -IEPOX,<sup>27</sup> and the relative amounts of  $\beta$ -[1,2]-INP to  $\beta$ -[4,3]-INP, we assign peak 1 to be all  $\delta$ -INHE isomers, and peak 4 and 5 to be *trans*- and *cis*- $\beta$ -[4,1]-INHE, which is formed from  $\beta$ -[1,2]-INP + OH. The *trans*- and *cis*- $\beta$ -[1,4]-INHE (produced from  $\beta$ -[4,3]-INP + OH) probably also forms, but likely the peaks are small and have the same elution time as peaks 6-8.

In experiment 8, chamber conditions were specifically altered to limit second-generation chemistry and OH formation in the dark. As expected, very little ISOPOOH (<100 ppt as an OH

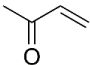
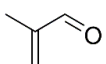
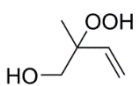
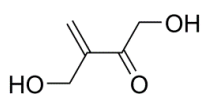
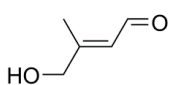
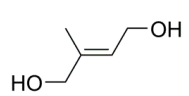
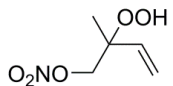
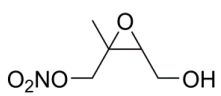
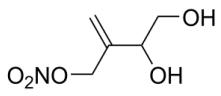
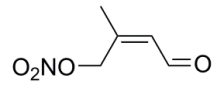
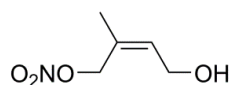
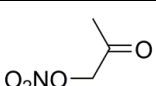
tracer) formed in the dark during this experiment, but peak 1 still represents approximately ~8% of the  $m/z = (-) 248$  signal. Very little INHE is predicted to form under dark conditions with low OH (Figure 2). Some of the  $\delta$ -INHE signal formed in the dark could be from  $\text{NO}_3$  reacting with IHN, but the reaction is slow and the yield is low (~13% if the chemistry is similar to what Jacobs et al. found for  $\beta$ -[4,3]-IHN + OH). The data suggests a first-generation product co-elutes with  $\delta$ -INHE.

Isoprene dihydroxy nitrate (IDHN), a product of the 1,5 H-shift of *trans*-[1,4]-INO (Scheme S3), is the most likely candidate for this first-generation product based on both its structure and expectation that it should form in relatively high yield. Furthermore, the percentage of IDHN and  $\delta$ -INHE to the entire  $m/z = (-) 248$  signal (18%, 6%, and 1%, in experiment 7, 8, and 10) decreased as the contribution of  $\text{RO}_2 + \text{RO}_2$  reactions decreased and other tracers for the [1,5]-H-shift reaction (IHCN and IHPN) decreased.

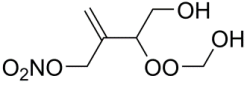
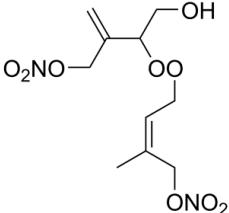
### **S3.0: PRODUCTS FORMED FROM $\text{NO}_3$ OXIDATION.**

Section 3.0 of the main work described the dominant products that form in the dark in experiment 8. The product yields for experiments 3-5 are included in Table S2 for comparison. Results from experiment 9 where the ToF-CIMS and the triple-CIMS were run together were used to estimate sensitivities for the triple-CIMS. As for the ToF-CIMS, the sensitivities for the triple-CIMS for all large nitrates ( $m/z \geq (-) 230$  except  $(-) 232$  and  $(-) 234$ , for which the ToF-CIMS sensitivity has been measured) are assumed to be the same as the triple-CIMS sensitivity for IHN. The sensitivities for the triple-CIMS changed over time depending on impurities in the system and other factors. A calibration system containing formic acid was used to account for changing sensitivities, so that experiments run at different times of the year could be compared. The sensitivities used in this study for the ToF-CIMS and triple-CIMS are listed in Table SA1.

**Table S2.** Yields for products formed during experiments 3-5 and experiment 8.

name	abbrev	structure	CIMS m/z	average yield expts 3-5 (%)	yield expt 8 (%)
<b>non-nitrates</b>					
methyl vinyl ketone	MVK		NA	0.090 <sup>A</sup>	<b>not measured</b>
methacrolein	MACR		NA	0.042 <sup>A</sup>	<b>not measured</b>
C <sub>5</sub> hydroxy hydroperoxide	ISOPOOH		(-) 203	0.02	0.007
C <sub>5</sub> dihydroxy carbonyl *	IDHC		(-) 201	0.019	0.032
C <sub>5</sub> hydroxy carbonyl	IHC		(-) 185	0.01	0.008
C <sub>5</sub> dihydroxy	IDH		(-) 187	0.006	0.006
<b>nitrates</b>					
C <sub>5</sub> nitrooxy hydroperoxide	INP		(-) 248	0.32	0.41
C <sub>5</sub> nitrooxy hydroxyepoxide	INHE				
C <sub>5</sub> dihydroxy nitrate	IDHN				
C <sub>5</sub> carbonylnitrate	ICN		(-) 230	0.26	0.12
C <sub>5</sub> hydroxynitrate	IHN		(-) 232	0.13	0.12
propanone nitrate	PROPNN		(-) 204	0.045	0.011

name	abbrev	structure	CIMS m/z	average yield expts 3-5 (%)	yield expt 8 (%)
C <sub>5</sub> hydroxy carbonyl nitrate	IHCN		(-) 246	0.029	0.021
C <sub>5</sub> hydroxy hydroperoxide nitrate	IHPN		(-) 264	0.028	0.032
isoprene dicarbonyl nitrate*	IDCN		(-) 244	0.015	0.008
unknown			(-) 261	0.015	0.005
ROOR from INO <sub>2</sub> and HMP and/or CIMS complex btw INP and CH <sub>2</sub> O*	INO2HM		(-) 278	0.01	0.017
C <sub>4</sub> carbonyl hydroxy nitrate	C4CHN		(-) 234	0.009	0.004
C <sub>4</sub> carbonyl hydroperoxy nitrate	C4CPN		(-) 250	0.006	0.005
ethanal nitrate	ETHLN		(-) 190	0.005	0.002
C <sub>5</sub> dinitrate	IDN		(-) 277	0.004	~ 0
C <sub>5</sub> carbonyl hydroperoxy nitrate	ICPN		(-) 262	0.003	0.001
ROOR from INO <sub>2</sub> and INO <sub>2</sub>	INO2IN		(-) 377	0.002	~ 0
C <sub>5</sub> dihydroperoxy nitrate	IDPN		(-) 280	0.002	0.002
C <sub>5</sub> dinitrooxy epoxide	IDNE		(-) 293	0.002	0.001

name	abbrev	structure	CIMS m/z	average yield expts 3-5 (%)	yield expt 8 (%)
ROOR from IHNO <sub>2</sub> and HMP and/or CIMS complex btw IHPN and CH <sub>2</sub> O	IHNO2HM		(-) 294	0.001	0.002
ROOR from INO <sub>2</sub> and IHNO <sub>2</sub>	hydroxy methyl peroxy INO2IHN		(-) 393	0.001	~ 0
			<b>totals</b>		
<b>non-nitrate sum</b>				<b>0.19</b>	<b>0.05<sup>B</sup></b>
<b>nitrate sum</b>				<b>0.89</b>	<b>0.76</b>
<b>total sum</b>				<b>1.08</b>	<b>0.81<sup>B</sup></b>

<sup>A</sup> A cold trap was only used for experiments 4-5, so MVK and MACR yields are only based on these experiments. <sup>B</sup> These yields do not include the yield for MVK and MACR as it was not measured for experiment 8. Abbreviation used are INO<sub>2</sub> (Isoprene nitrooxy peroxy radical), IHNO<sub>2</sub> (Isoprene hydroxy nitrooxy peroxy radical from 1,5 H shift see Section S3.1), and HMP (hydroxy methyl peroxy). Yields for experiments 3-5 and experiment 8 were calculated 4 h and 2.5h after isoprene injection, respectively. \* Assignment of this compound is less certain. A compound with a different/unknown structure could also be present.

Based on the GC-ToF-CIMS results, INP is fragmenting in the CF<sub>3</sub>O<sup>-</sup> CIMS to a number of products detected at m/z = (-) 59, (-) 63, (-) 81, (-) 118, (-) 202, (-) 209, (-) 225, (-) 228, and (-) 230. Results for experiment 7, which had the highest amount of INP formed, were used to calculate the degree of fragmentation for all fragments except for m/z = (-) 230. Experiment 8, which had higher resolution results, was used to calculate the fragmentation for m/z = (-) 230. Only products with a transmission less than ~100% and elution time similar to INP were included. β-INP (~20%) fragmented more than δ-INP (~9%). The degree of fragmentation was used to correct the overall β to δ ratio determined by the GC-CIMS. If the ratio of β- to δ-INP is similar to this study, ~12% of INP fragments.

Some products had much higher transmissions, but they were not included because fragmentation could be occurring in the CIMS or on the column. It is also possible that INP fragments into products we cannot detect (e.g., MVK and MACR). Additionally,  $m/z = (-) 278$  could be a complex of INP and  $\text{CH}_2\text{O}$  in the  $\text{CF}_3\text{O}^-$  CIMS, but the transmission of  $m/z = (-) 278$  through the 1m and 4m columns is only  $\sim 70\%$  and  $\sim 40\%$ , respectively. We would expect the transmission to be zero if  $m/z = (-) 278$  is all a complex on the CIMS. We do not include a correction for this, but if all of the  $m/z = (-) 278$  not transmitting through the column is a complex of INP and  $\text{CH}_2\text{O}$ , this would increase the INP signal in experiment 8 by  $\sim 2\%$ . Part of the  $(-) 278$  signal is likely the ROOR product from  $\text{INO}_2 + \text{hydroxy methyl peroxy radical (HMP)}$ . However, the  $m/z = (-) 278$  signal is too high to be explained entirely by the two pathways above suggesting there is another pathway for its formation as well (see S4.3 for more possibilities).

$\sim 5\%$  of INP fragments in the ToF-CIMS to form  $m/z = (-) 230$ . We know from experiment 9 that  $\sim 16\%$  of INP fragments in the triple-CIMS to form  $m/z = (-) 230$ . The experimental data in Table S2 for INP and ICN were corrected based on this fragmentation. A GC is not attached to the triple-CIMS used in experiments 1-6, so INP should be taken as a lower limit for these experiments, as other fragmentation products likely form, but a correction cannot be measured.

The estimated sensitivities are the largest source of error for these experiments. The estimated total error for the triple-CIMS, a combination of the error in ToF-sensitivities ( $\pm 20\%$ ) and the non-direct triple calibration ( $\pm 15\%$ ), is approximately  $\pm 35\%$  for compounds in which the ToF sensitivities are understood ( $m/z < (-) 230$  and  $(-) 232$ , and  $(-) 234$ ). For the large nitrates ( $m/z \geq (-) 230$  except  $(-) 234$  and  $(-) 232$ ) the errors could be larger because no synthetic standards are

available to calibrate the instruments, but we do not expect the errors to be much greater than  $\pm 35\%$ .

Two compounds at  $m/z = (-) 201$  and  $(-) 244$  form in the dark, but we are not able to define a chemical mechanism consistent with the production of compounds at these masses. During the BEARPEX field campaign  $m/z = (-) 244$  formed at night, so this product is likely atmospherically relevant.<sup>35</sup> Both products may form in a minor yield from reactions of  $\text{INO}_2$ ,  $\text{IHNO}_2$  or  $\text{IPNO}_2$  with  $\text{HO}_2$  or  $\text{RO}_2$ .

**S3.1 Proposed RO [1-5] Hydrogen Shift Products.** Kwan et al.<sup>7</sup> and Ng et al.<sup>36</sup> proposed the formation of products from the [1,5]-H-shift of *trans*-[1,4]-INO and *cis*-[1,4]-INO, respectively (Scheme S3). We expect that the peroxy radical ( $\text{IHNO}_2$ ) that forms from the [1,5]-H-shift of the *trans*-[1,4]-INO will react with  $\text{HO}_2$  and form only the  $\text{C}_5$  hydroxy hydroperoxy nitrate (IHPN) given that only acetylperoxy radicals and  $\alpha$ -carbonyl peroxy radicals have been shown to produce OH.<sup>37</sup> Both resonance structures of IHPN have the nitrate group further removed from the peroxy radical. However, more studies measuring OH yields from functionalized nitrooxy peroxy radicals need to be conducted to confirm this assumption.  $\text{C}_5$  hydroxy carbonyl will form from the [1,5]-H-shift of *cis*-[1,4]-INO radical (Scheme S3) and isoprene + OH chemistry, so we do not try to estimate a rate constant for this [1,5]-H-shift. However, we expect the H-shift of the *cis*-[1,4]-INO radical to be slower because hydrogen abstraction occurs more slowly for carbons adjacent to a nitrate group.<sup>10</sup>



**Scheme S3.** Main products proposed for the [1,5]-H-shift of (a) *trans*-[1,4]-INO, and (b) *cis*-[1,4]-INO<sup>36</sup>. For brevity, products from only the dominant resonance structure are shown.

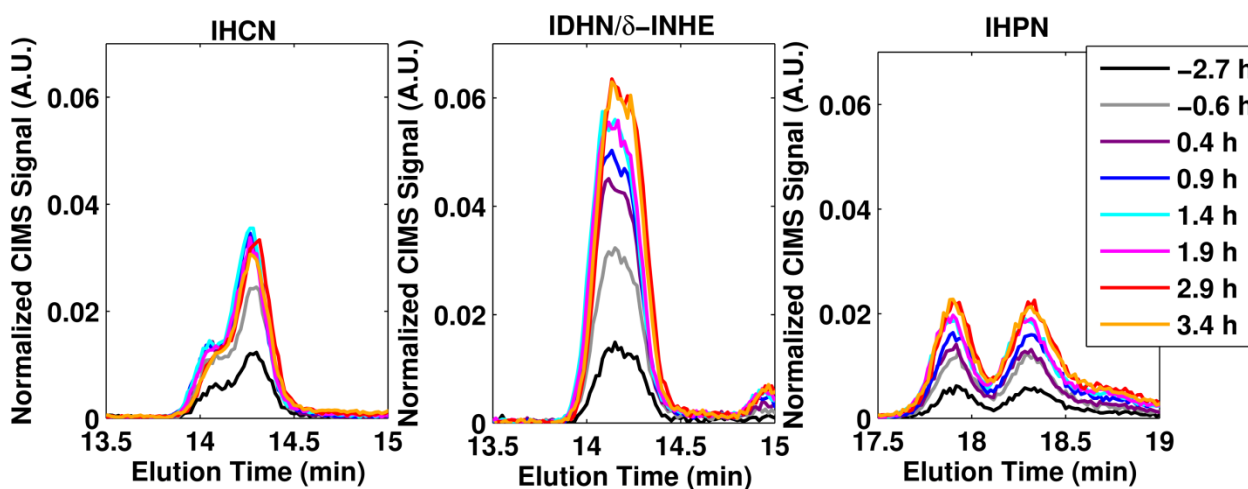
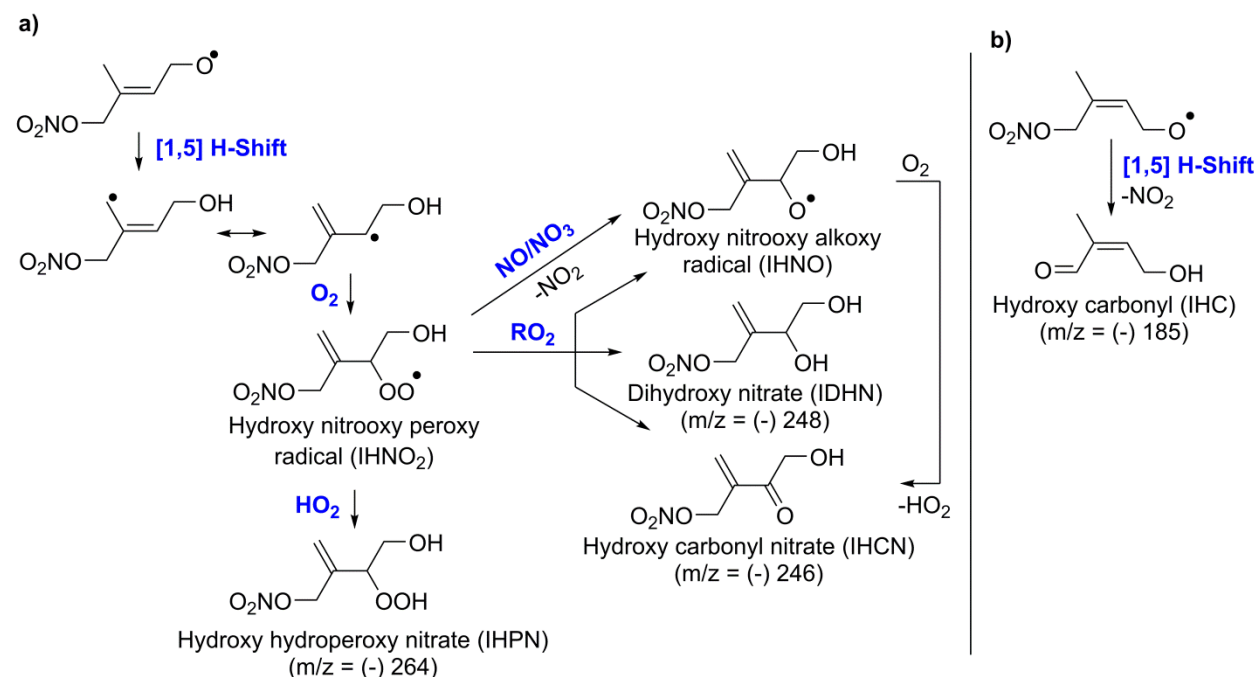


**Figure S2.** GC-ToF-CIMS chromatographs for C<sub>5</sub> hydroxy carbonyl nitrate (IHCN), C<sub>5</sub> dihydroxy nitrate (IDHN)/ $\delta$ -INHE, and C<sub>5</sub> hydroxy hydroperoxy nitrate (IHPN) as a function of time since photochemistry initiation. Signals for IHPN were increased by 25% to account for low transmission in the 4m column.

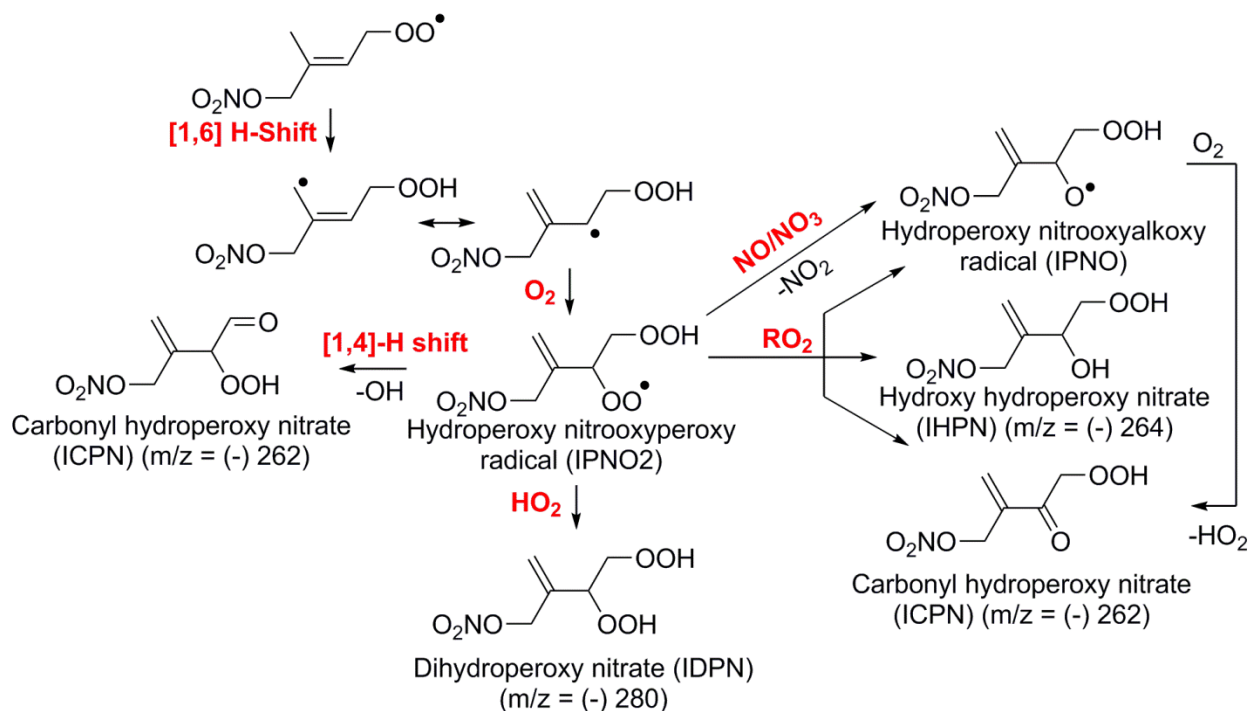
As discussed in Section S2.0, IDHN and  $\delta$ -INHE co-elute. In order to estimate the amount of IDHN present in the experiments we have included the [1,5]-H-shift of the *trans*-[1,4]-INO into the kinetic mechanism. A general  $k_{[1,5]\text{-H-shift}} = \sim 2 \times 10^5 \text{ s}^{-1}$  and increasing all  $k_{\text{IHNO}_2 + \text{RO}_2}$  (except  $k_{\text{IHNO}_2}$ ) by 2-fold best fit the experimental data for experiment 5. Peeters et al.<sup>38</sup> found that C<sub>5</sub> carbonyl alkoxy radicals (produced from the photolysis of C<sub>5</sub> hydroperoxy aldehydes (HPALDs)) rapidly interconvert between the *cis* and *trans* states. Assuming a similar interconversion occurs for the nitrooxy alkoxy radicals and that most of the INO in this study comes from RO<sub>2</sub> + RO<sub>2</sub> chemistry, we use the  $\delta$ -[1,4] distribution (0.73) in Table 4, Column 2 to adjust the rate constant to account for only the [1,4]-INO undergoing the shift ( $\sim 3 \times 10^5 \text{ s}^{-1}$ ). Not many [1,5]-H-shift rate constants have been measured. The isomerization rate constants for n-butoxy ( $2.4 \times 10^5 \text{ s}^{-1}$ ) and 2-pentoxo radicals ( $3.0 \times 10^5 \text{ s}^{-1}$ )<sup>39</sup> are close to the adjusted rate constant.

Although the oxidation of IHPN by OH might be expected to form an epoxide, there is no clear evidence suggesting this occurs. In experiment 7, there was 100% transmission of  $m/z = (-) 264$  throughout the experiment, and no new peak formed after photooxidation. It is possible that the epoxide formed, but quick wall and lines losses prevented detection by the CIMS.

**S3.2 Proposed RO<sub>2</sub> [1-6] Hydrogen Shift Products.** Given the formation in the dark of ICPN ( $m/z = (-) 262$ ) and IDPN ( $m/z = (-) 280$ ), we suspect that the *trans*-[1,4]-INO<sub>2</sub> isomer will undergo a [1,6]-hydrogen shift (Scheme S4). Both of these signals increased only when isoprene was present in the chamber, suggesting they are first-generation products. We inferred rate constants using the kinetic mechanism and results for experiment 5. There are two pathways in this system to form isoprene carbonyl hydroperoxy nitrate (ICPN). For simplicity,  $k_{\text{IPNO}_2 + \text{RO}_2}$

(except IHO<sub>2</sub>) was increased by the same factor (2) as  $k_{\text{IHNO}_2 + \text{RO}_2}$  (except IHO<sub>2</sub>), and the rest of the ICPN signal was assumed to be from the [1,4]-H shift.

**Scheme S4.** Main products formed from the [1,6]-H-shift of *trans*-[1,4]-INO<sub>2</sub>. For simplicity, products from only the dominant resonance structure are shown.



The [1,6]-H-shift rate constant that best fits with the experimental results is  $\sim 4 \times 10^{-4} \text{ s}^{-1}$ . To account for only one isomer isomerizing, the INO<sub>2</sub> distribution determined in Table 5 is used together with the assumption that an equal amount of *trans* and *cis* isomers form, to scale the [1,6]-H-shift rate constant to  $\sim 2 \times 10^{-3} \text{ s}^{-1}$ . The  $k_{[1,4]\text{-H-shift}}$  that best fit experimental results is  $\sim 2 \times 10^{-2} \text{ s}^{-1}$  which, as expected, is less than the  $k_{[1,5]\text{-H-shift}}$  ( $> 0.1 \text{ s}^{-1}$ ) determined by Crounse et al.<sup>21</sup> for a similar compound. Recall, however, that all of the ICPN product may be explained by a greater  $k_{\text{IPNO}_2 + \text{RO}_2}$ . It is also possible to form ICPN and IDPN by other means (e.g., the [1,4]-H-shift of IHNO<sub>2</sub> also could form ICPN), so the above rate constant and subsequent branching ratios are only upper limits/rough estimates and need to be verified using a simpler system.

Nevertheless, the RO<sub>2</sub> lifetime at night is often much longer than that during the day, so this chemistry could be quite important in the ambient atmosphere and deserves further study.

#### **S4.0 AEROSOL UPTAKE.**

**S4.1 INHE Uptake into Highly-Acidified Seed.** After INHE formation in experiments 3, we injected highly-acidified seed particles under low RH conditions (particle pH <0, particle water content ~10-30% by volume due to H<sub>2</sub>SO<sub>4</sub> hygroscopicity<sup>40</sup>) to more-clearly demonstrate uptake. We note that this was done to diagnose that INHE is surface active; it is not meant to be representative of atmospheric heterogeneous chemistry.

When highly acidic MgSO<sub>4</sub> + H<sub>2</sub>SO<sub>4</sub> seed was atomized into the chamber, INHE declined in the gas phase (Figure S3a) and the total organic increased in the particle phase (Figure S3b). The particle growth demonstrates that, like other epoxides,<sup>34, 41</sup> INHE efficiently undergoes reactive uptake to wet acidified aerosol. The gas-phase loss is likely due to the combination of uptake onto wet acidic seeds and irreversible losses to acidic chamber walls.

At the time of seed injection for experiments 1-5, most of the CIMS signal at m/z = (-) 248 is carried by INHE. The kinetic mechanism predicts that INP, IDHN, and INHE make up 1%, 15%, and 83%, respectively, of the m/z = (-) 248 signal. The (-) 63 daughter characteristic of organic peroxides is no longer being produced in MS/MS mode from m/z = (-) 248. Although only  $\beta$ -INP isomers efficiently produce the (-) 63 daughter in MS/MS mode, we expect that concentrations of  $\delta$ -INP are also minimal as they react with OH faster than  $\beta$ -INP.

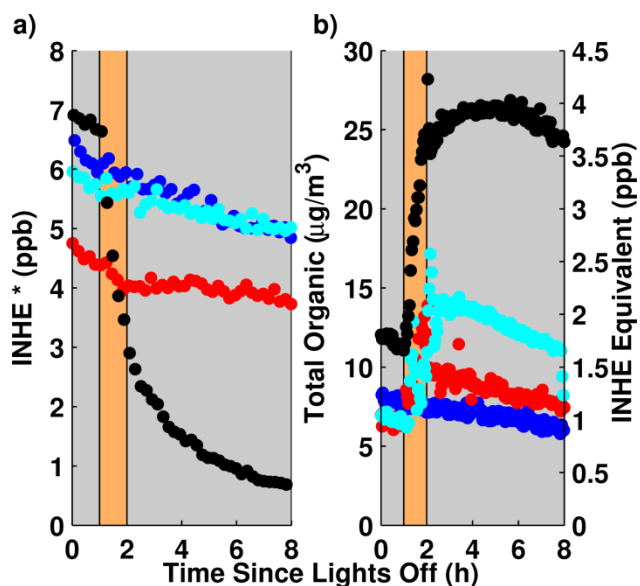


**Figure S3.** (a) INHE gas phase loss detected by CIMS and (b) total organic mass growth detected by the AMS for dry and no seed (blue), dry (NH<sub>4</sub>)<sub>2</sub>SO<sub>4</sub> (red), hydrated (NH<sub>4</sub>)<sub>2</sub>SO<sub>4</sub> (cyan), and hydrated MgSO<sub>4</sub>·H<sub>2</sub>SO<sub>4</sub> (black). \*This signal also includes a small fraction IDHN and INP. The tan region indicates when seed was injected. On the right hand axis of panel b, total organic is converted to INHE (ppb) for clarity.

Lin et al.<sup>42</sup> identified the following AMS tracers for IEPOX: C<sub>4</sub>H<sub>5</sub><sup>+</sup>, C<sub>5</sub>H<sub>6</sub>O<sup>+</sup>, C<sub>3</sub>H<sub>7</sub>O<sub>2</sub><sup>+</sup>, and C<sub>5</sub>H<sub>8</sub>O<sub>2</sub><sup>+</sup>. These same tracers increase significantly when highly acidic seed is injected into the chamber both during experiment 3 and 6 (Figure S4 and S5), but not for the other seed types. When particles were injected in these experiments, there was only ~0.3 and ~0.1 ppb of IEPOX, so IEPOX was not the main source of these ions. The main source of these fragments is likely INHE for experiment 3 and IDHN for experiment 6.

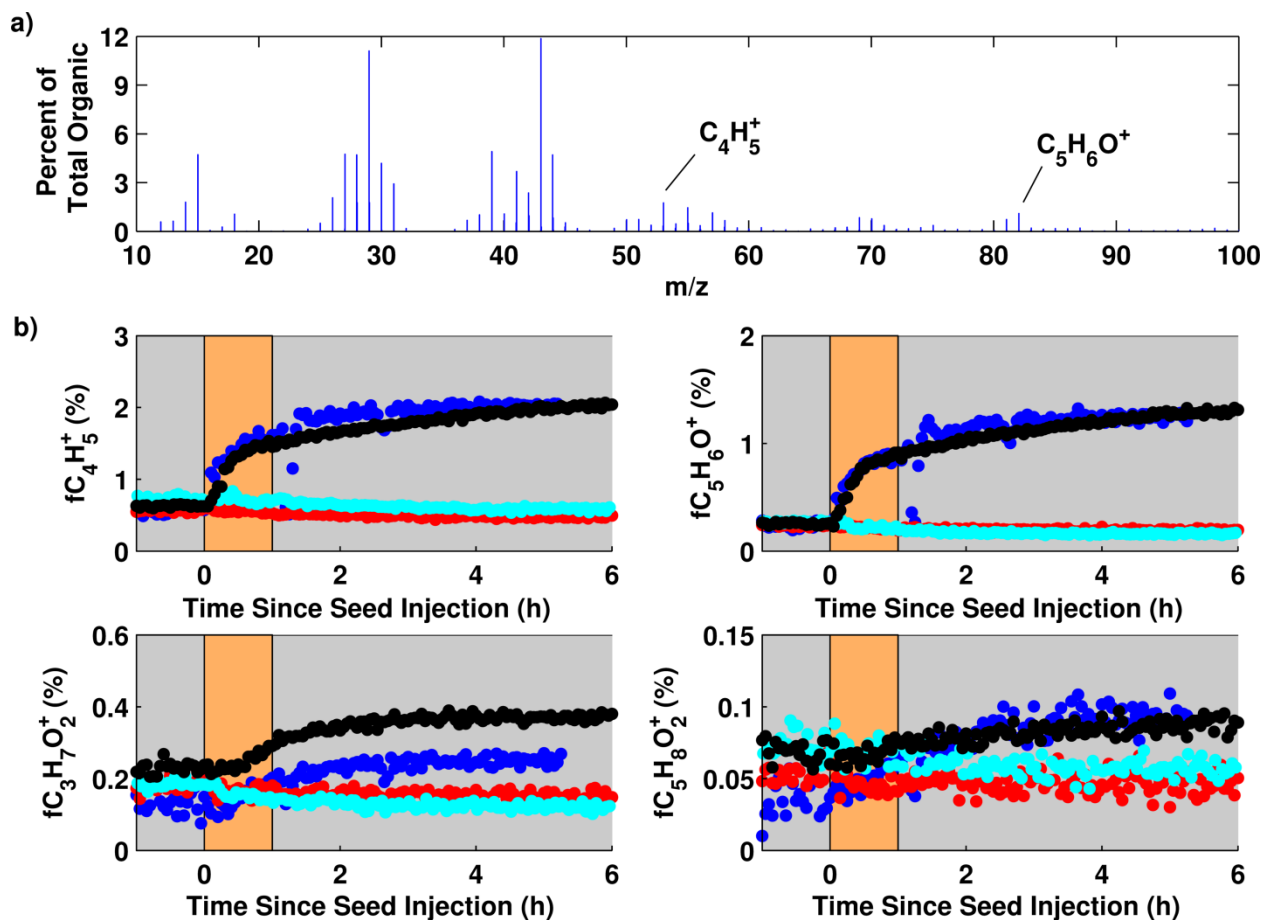


**Figure S4.** (a) AMS spectrum (percent of total organic) for hydrated  $MgSO_4:H_2SO_4$  (1:1) seed at peak growth. (b) AMS fragments (percent of total organic) proposed to be tracers for IEPOX<sup>42</sup> for hydrated  $MgSO_4:H_2SO_4$  seed before photooxidation (blue), dry  $(NH_4)_2SO_4$  seed (red), hydrated  $(NH_4)_2SO_4$  seed (cyan), and hydrated  $MgSO_4:H_2SO_4$  seed after photooxidation (black). Tan region indicates when seed was injected.

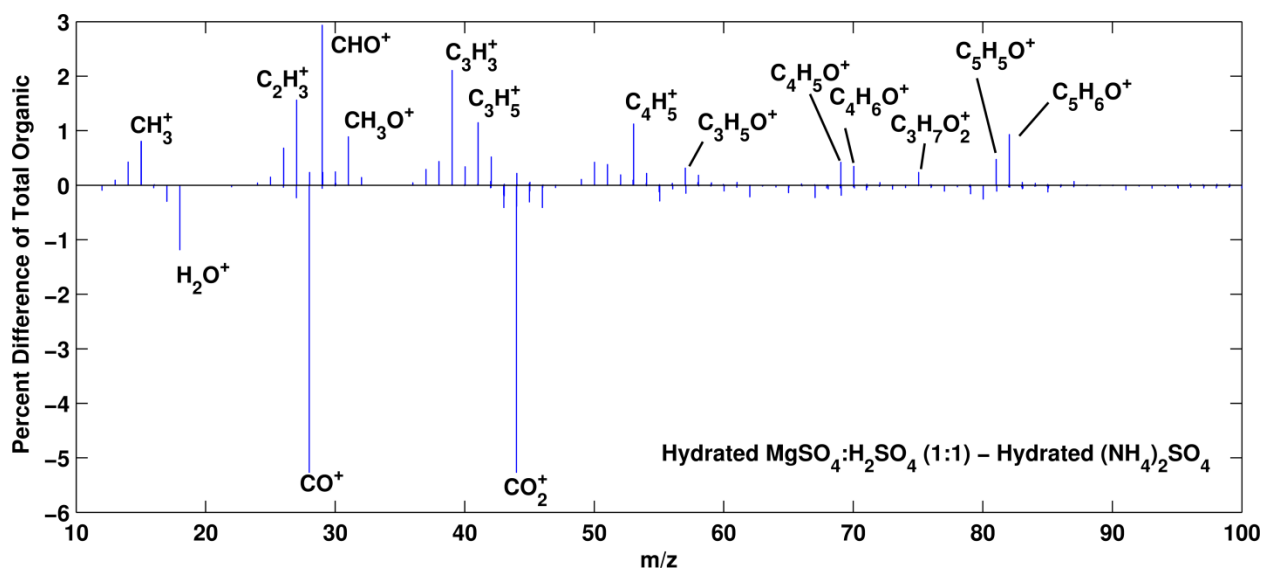


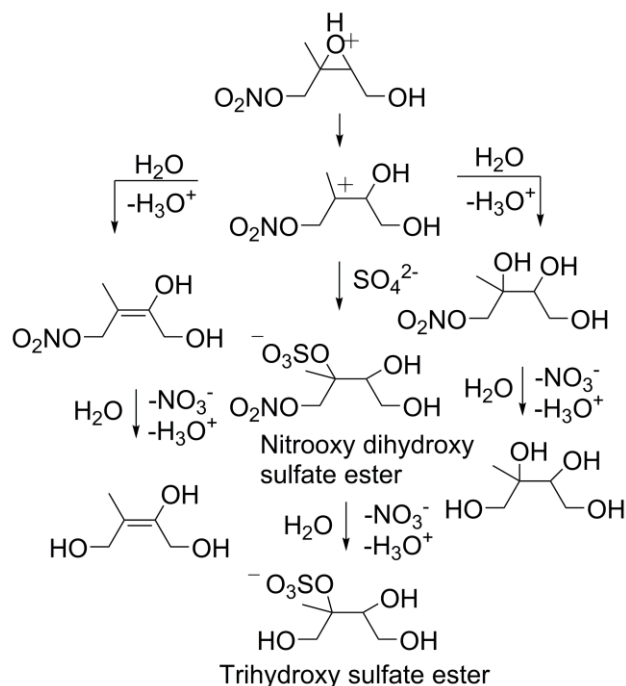
**Figure S5.** AMS difference spectrum (percent of total organic) between hydrated  $\text{MgSO}_4\cdot\text{H}_2\text{SO}_4$  (1:1) and hydrated  $(\text{NH}_4)_2\text{SO}_4$  seed.

We verify that lingering IEPOX,  $\sim 0.3$  ppb (experiment 3) and  $\sim 0.1$  ppb (experiment 6), present during seed injection, contributes to these signals only to a small degree. In experiment 3 where IEPOX had the highest concentration, INHE declined on the CIMS by  $\sim 40 \mu\text{g}/\text{m}^3$ . Other compounds also declined including hydroxy methyl hydroperoxide,  $\text{C}_5$  carbonyl hydroxy epoxide, IEPOX,  $\text{C}_5$  hydroxy hydroperoxy epoxide,  $\text{C}_4$  nitrooxycarbonyl hydroperoxide, and  $\text{C}_5$  hydroxy hydroperoxide nitrate. These other compounds made up an additional  $\sim 30 \mu\text{g}/\text{m}^3$  as determined by the decline in the CIMS signal. We assume IEPOX fragments on the AMS as measured by *cis*- and *trans*-IEPOX standards by Nguyen et al.<sup>43</sup>, and that the ratio of *cis* and *trans*-IEPOX formed is similar to that measured by Bates et al.<sup>27</sup>. After seed injection, the AMS signal increased by  $\sim 15 \mu\text{g}/\text{m}^3$ , so the worst case the adjusted  $f_{\text{C}_5\text{H}_6\text{O}^+}$  fragment becomes 1.0% and best case 1.3%. Both cases are well above what is considered background signal for  $f_{\text{C}_5\text{H}_6\text{O}^+}$ .<sup>44</sup>

There are two possibilities for why AMS tracers for heterogeneous uptake of INHE and IDHN are similar to those for IEPOX. In the  $\text{MgSO}_4 + \text{H}_2\text{SO}_4$  seeds, the nitrate group is known to be easily hydrolyzed<sup>15, 45-46</sup> yielding tetrols and organic sulfates identical to those produced from IEPOX<sup>41</sup> (Scheme S5). If correct, these AMS tracers will only reflect INHE/IDHN uptake when the nitrate groups are hydrolyzed. Under less acidic conditions, reactive uptake of INHE may still occur, but different products are formed, which would have different fragmentation patterns on the AMS (e.g., INHE-derived dinitrate if nitric acid also partitions as is the case here). This implies that INHE undergoes reactive uptake to both hydrated  $(\text{NH}_4)_2\text{SO}_4$  and acidic sulfate, similarly to IEPOX<sup>34, 41, 43</sup>. Alternatively, it is possible that the AMS fragments INHE/IDHN-derived compounds in a similar manner to IEPOX-derived compounds (i.e., the nitrate group does not greatly impact the fractionation pattern). If this is true, it implies that INHE does not undergo reactive uptake to seed types less acidic than  $\text{MgSO}_4\text{:H}_2\text{SO}_4$  seed because IEPOX AMS tracers do not increase for the dry or hydrated  $(\text{NH}_4)_2\text{SO}_4$  seeds.



**Scheme S5.** Proposed products of  $\beta$ -[4,1]-INHE that form in the particle phase under hydrated acidic conditions.



From this study, we conclude that in acidic atmospheric aerosols, uptake of INHE/IDHN will yield the AMS tracers  $C_4H_5^+$ ,  $C_5H_6O^+$ ,  $C_3H_7O_2^+$ , and  $C_5H_8O_2^+$  that are clearly not unique to IEPOX. Indeed, Ng et al.<sup>36</sup> using UPLC/(-)ESI-TOFMS detected trihydroxy sulfate ester and nitrooxy dihydroxy sulfate ester (Scheme S5) in SOA generated during isoprene  $NO_3$  oxidation chamber experiments with highly acidic seed. Ng et al. note that these products have been previously detected in field studies as organosulfates produced from isoprene photooxidation.<sup>47-</sup>

48

Hatch et al.<sup>49</sup> using ATOFMS during the ANARChE and AMIGAS field campaigns found that trihydroxy sulfate ester increased at night and is well correlated with  $NO_x$  emissions. It is possible that in this study, some of the trihydroxy sulfate ester attributed to IEPOX reflected

uptake of INHE/IDHN instead. The chemistry described in the present study could be a direct link for nighttime SOA formation from isoprene.

**S4.2 Potential INHE Uptake into Hydrated  $(\text{NH}_4)_2\text{SO}_4$  Seed.** Nguyen et al.<sup>43</sup> found that *cis* and *trans*- $\beta$ -IEPOX undergoes reactive uptake to hydrated  $(\text{NH}_4)_2\text{SO}_4$  seed aerosol. By analogy, IHNE should also undergo reactive uptake to aqueous seeds, but our results are inconclusive, and further work is needed as hydrated  $(\text{NH}_4)_2\text{SO}_4$  seeds are expected to be important in the lower troposphere. There is an increase in the total organic mass for hydrated  $(\text{NH}_4)_2\text{SO}_4$  (RH ~42% at seed injection) versus dry  $(\text{NH}_4)_2\text{SO}_4$  (Figure S3b, cyan markers) that equals ~ half the organic mass of the experiment using highly-acidified seeds (Figure S3b, black markers). Thus, hydrated  $(\text{NH}_4)_2\text{SO}_4$  seeds clearly produce SOA from the partitioning of organic compounds in this reaction. However, the CIMS signal for INHE for dry and hydrated  $(\text{NH}_4)_2\text{SO}_4$  experiments looks similar, and without a corresponding net decay of the INHE signal, it is not possible to implicate this epoxide in the reactive uptake. Even though  $\sim 300 \mu\text{g m}^{-3}$  of seed was added, the surface area of the chamber walls is still ~ 200 times greater than the surface area of the particles. Unless the particles represent a very different surface chemically than the walls (e.g., highly acidic seeds), the decline in the gas phase from any seed addition will be masked by wall deposition, so the CIMS signal is unlikely to change substantially when seed is injected.

The O:C and N:C ratios of the nucleated aerosol prior to seed injection for all of the experiments are fairly similar (red markers in Figure S6). The O:C ratio decreased rapidly for the highly acidic seed, and increased slightly for the dry and hydrated  $(\text{NH}_4)_2\text{SO}_4$  seeds. One possible explanation for why the O:C ratio decreases for the acidic seed case is that after injection, gas-phase products undergo reactive uptake to the acidic seed. The O:C ratio of these gas-phase products is likely lower than that of the organic aerosol formed prior to seed addition.

The N:C ratio grew appreciably for only the hydrated  $(\text{NH}_4)_2\text{SO}_4$  seeds. There are three possible explanations. The CIMS signal for nitric acid dropped significantly ( $\sim 90$  ppb), only when hydrated  $(\text{NH}_4)_2\text{SO}_4$  seed was injected into the chamber. This nitric acid can react with organic species in the particle phase to form organonitrates, reactive uptake of nitrates present in the gas phase can occur, or there may be organic amine formation from the epoxide.<sup>43</sup> In the present system it is not possible to determine which scenario is dominant. Figure S6 demonstrates that the chemical nature of the particles depends greatly on the relative humidity and seed type.

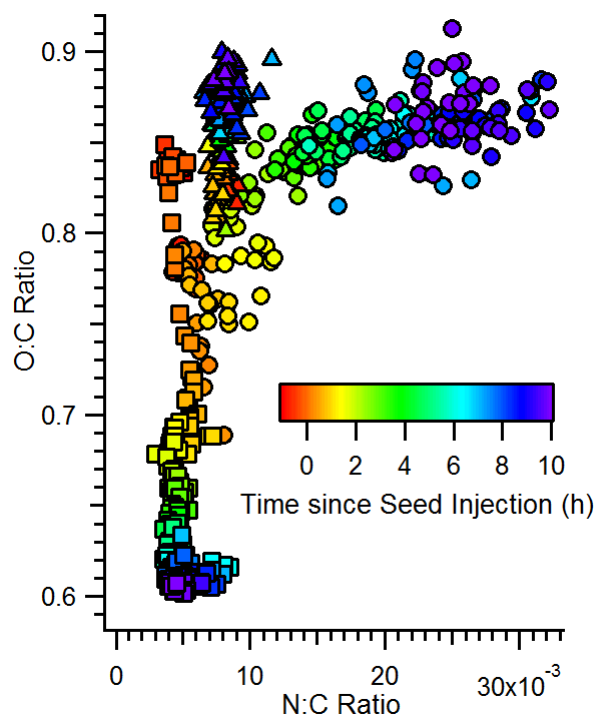


**Figure S6.** Change in N:C and O:C ratios for hydrated  $(\text{NH}_4)_2\text{SO}_4$  seeds (circles), hydrated  $\text{MgSO}_4 + \text{H}_2\text{SO}_4$  seeds (squares), and dry  $(\text{NH}_4)_2\text{SO}_4$  seeds (triangles).

Hydrolysis of primary  $\delta$ -hydroxy nitrates was thought to be slow in neutral solutions ( $\tau > 2500$  h).<sup>45</sup> Very acidic conditions (55 wt%  $\text{D}_2\text{SO}_4$ ) were needed for the loss rate to be reasonably fast ( $\tau = 1.7$ -2.5 h),<sup>46</sup> and such high acidities are unlikely to occur in the ambient atmosphere. Jacobs et al.<sup>15</sup>, however, measured the neutral hydrolysis lifetimes of  $\delta$ -[1,4N]-IHN and  $\beta$ -[4,3N]-IHN to

be 2.46 min and 17.5 h, respectively, and suggested the neutral hydrolysis lifetimes of these nitrates are much faster than equivalent saturated hydroxy nitrates because of the allylic character of their transition states. Many of the isomers of INP, IHN, and ICN also have transition states of an allylic nature, so we anticipate that their hydrolysis rates may also be fast (although the influence of a carbonyl or hydropoxide substituent on hydrolysis rate constants is unknown). Thus, hydrolysis of the  $\delta$  isomers produced in the  $\text{NO}_3$  chemistry may be important in the atmosphere, especially for regions with high RH.

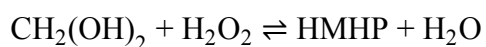
After seed injection, products partitioning to the gas phase from the particle phase are quite different depending on whether hydrated non-acidified seed or hydrated highly acidic seed is injected, implying that there is very different chemistry occurring in the two conditions. Some of the chemistry is likely similar between the two cases. For example, for both seed types, glycolaldehyde was produced in the particle phase in sufficient quantities to partition to the gas phase several hours after seed injection. There are also differences as well. For instance, several hours after hydrated  $(\text{NH}_4)_2\text{SO}_4$  was injected into the chamber the signal for  $\text{H}_2\text{O}_2$  increased, but this did not happen during the high RH no seed experiment or for any other seed types. This suggests that either  $\text{H}_2\text{O}_2$  or precursors to  $\text{H}_2\text{O}_2$  (i.e.,  $\text{HO}_2$  or  $\text{OH}$ ) formed in the particle phase and partitioned to the gas phase. Understanding this chemistry may be important for accurately simulating the  $\text{HO}_x$  cycle in atmospheric models.  $\text{H}_2\text{O}_2$  has unique chemistry in the hydrated  $(\text{NH}_4)_2\text{SO}_4$  case, which is the most atmospherically relevant, and highlights the importance of running chamber experiments under high RH conditions.

Jacobs et al.<sup>15</sup> found that [4,3N]-IHN oxidation by  $\text{OH}$  produced a 13% yield of IEPOX at 760 torr and proposed that this chemistry likely occurs for many compounds where an alkyl radical is adjacent to a nitrate group. In these experiments, there was a slight increase in the mass signals

for these epoxides when photooxidation began and OH added to the double bond in ICN and INP. Like other epoxides, these signals decline when hydrated highly acidic seed particles are injected into the chamber, but not when  $(\text{NH}_4)_2\text{SO}_4$  seed particles are injected at low RH.

During the high RH experiments, wall deposition of hydroxyl methylperoxyl radical (HMP) and IHPN was sufficiently high that none of the products remained in the gas phase by the time seed was injected into the chamber. HMP and IHPN also decayed quickly when hydrated highly acidic seed was injected in experiments 3 and 6.

**S4.3 Potential Influence of  $\text{CH}_2\text{O}$ .** Because  $\text{CH}_2\text{O}$  was used in high quantities in these experiments, it is important to determine its influence on the particle phase chemistry. The products that form can also help determine the types of reactions expected to occur in the atmosphere.  $\text{CH}_2\text{O}$  in aqueous solution exists mostly in the hydrated form (i.e.,  $\text{CH}_2(\text{OH})_2$ ). In experiments 1 and 2 when the RH is  $\sim 40\%$ ,  $\text{CH}_2(\text{OH})_2$  ( $m/z = 133$ ) increased as soon as  $\text{CH}_2\text{O}$  was injected into the chamber.  $\text{CH}_2\text{O}$  likely reacted with water present on the walls and some of the  $\text{CH}_2(\text{OH})_2$  partitioned back to the gas phase.  $\text{CH}_2(\text{OH})_2$  also formed in the low RH experiments, but with a much smaller yield. The following equilibria have been identified for  $\text{CH}_2(\text{OH})_2$  in the aqueous phase<sup>50</sup>, where BHMP is  $\text{HOCH}_2\text{O}_2\text{CH}_2\text{OH}$ :



Immediately after seed injection, HMHP declined in both experiments 3 and 6, but BHMP and  $\text{CH}_2(\text{OH})_2$  increased only in experiment 6. This implies that for the conditions of experiment 6,  $\text{CH}_2\text{O}$  partitions to the particle phase.  $\text{MgSO}_4$  &  $\text{H}_2\text{SO}_4$  seed is acidic enough to attract water, and  $\text{CH}_2(\text{OH})_2$  reacts with HMHP in the particle phase to form BHMP, some of which partitioned to the gas phase.

Since Marklund<sup>50</sup> found that HMHP reacts with  $\text{CH}_2(\text{OH})_2$ , it is possible that other hydroperoxides will react with  $\text{CH}_2(\text{OH})_2$  in a similar manner. In experiment 6, when  $\text{MgSO}_4\&\text{H}_2\text{SO}_4$  seed aerosol was added to the chamber, a small amount of  $m/z = (-) 233$ ,  $(-) 278$  and  $(-) 294$  was produced slowly. These signals are potentially the ROOR formed from ISOPOOH, INP and IHPN reacting with  $\text{CH}_2(\text{OH})_2$  in the particle-phase. We see  $m/z = (-) 278$  rising much more than we would expect due to ROOR formation from  $\text{RO}_2 + \text{RO}_2$  gas-phase reactions. It is possible that these ROOR form on the walls and repartition in a small degree back to the gas-phase. In experiment 3,  $m/z = (-) 233$  and  $(-) 278$  also grew when  $\text{MgSO}_4\&\text{H}_2\text{SO}_4$  seed was added, but ISOPOOH and INP are not expected to undergo reactive uptake to the  $\text{MgSO}_4\&\text{H}_2\text{SO}_4$ . Possibly  $m/z = (-) 233$  and  $(-) 278$  are IEPOX and INHE ring opening in acidic conditions and reacting with  $\text{CH}_2\text{O}$  to form diaxolane-type compounds.<sup>51</sup> This chemistry is highly speculative, but deserves further study.

The formation of these  $\text{CH}_2\text{O}$  and nitrate dimers seems to be acid catalyzed since these products are not detected in the gas phase when other seed types were added into the chamber. However, our understanding is limited to the products that partition back to the gas-phase. These dimer species could also have been present in the hydrated  $(\text{NH}_4)_2\text{SO}_4$  seed, but the larger activity of water prevented them from partitioning out of the particle phase or the dimers formed more slowly and never accumulated sufficiently in the gas phase in order to be detected by the CIMS. Understanding this effect will be important for future aerosol yield studies if  $\text{CH}_2\text{O}$  is used to generate  $\text{HO}_2$ . However, if these dimer products form under all conditions, they are unlikely to alter the yield significantly since  $\text{CH}_2\text{O}$  has such a low mass. Because we see these dimers form only under highly acidic conditions, the yields determined from dry or hydrated  $(\text{NH}_4)_2\text{SO}_4$  seeds will likely not be affected by this chemistry.

## APPENDIX

**Table SA1.** Sensitivities used in this study for the triple-CIMS (experiments 3-5) and ToF-CIMS.

name	CIMS m/z	Triple-CIMS sensitivity (normcts/ppt)	ToF-CIMS sensitivity (normcts/ppt)
formic acid	(-) 65	$2.0 \times 10^{-5} \text{ }^A$	$1.0 \times 10^{-4} \text{ }^A$
nitric acid	(-) 82	$9.1 \times 10^{-5} \text{ }^A$	$3.9 \times 10^{-4} \text{ }^A$
H <sub>2</sub> O <sub>2</sub>	(-) 119	$1.1 \times 10^{-4} \text{ }^A$	$1.5 \times 10^{-4} \text{ }^A$
hydroxy methyl hydroperoxide	(-) 149	$4.5 \times 10^{-5}$	NA
C <sub>5</sub> hydroxy carbonyl	(-) 185	$9.5 \times 10^{-5}$	$2.0 \times 10^{-4}$
C <sub>5</sub> dihydroxy	(-) 187	$9.5 \times 10^{-5}$	$2.0 \times 10^{-4}$
C <sub>5</sub> dihydroxy carbonyl	(-) 201	$8.9 \times 10^{-5}$	$1.4 \times 10^{-4}$
C <sub>5</sub> carbonyl hydroxy epoxide	(-) 201	Assume same as IEPOX	NA
ISOPOOH/IEPOX	(-) 203	$1.1 \times 10^{-4} \text{ }^A$	$1.6 \times 10^{-4}$
ethanal nitrate	(-) 190	$2.2 \times 10^{-4}$	$3.6 \times 10^{-4}$
propanone nitrate	(-) 204	$1.9 \times 10^{-4}$	$3.1 \times 10^{-4}$
C <sub>5</sub> hydroxy hydroperoxy epoxide	(-) 217	Assume same as IEPOX	NA
IHN	(-) 232	$2.6 \times 10^{-4}$	$3.6 \times 10^{-4}$
C <sub>4</sub> carbonyl hydroxy nitrate	(-) 234	$2.2 \times 10^{-4}$	$3.3 \times 10^{-4}$
INP/INHE	(-) 248	$2.6 \times 10^{-4}$	$3.6 \times 10^{-4}$
ICN	(-) 230		
C <sub>5</sub> dicarbonyl nitrate	(-) 244		
C <sub>5</sub> hydroxy carbonyl nitrate	(-) 246		
C <sub>4</sub> nitrooxycarbonyl hydroperoxide	(-) 250		
unknown	(-) 261		
C <sub>5</sub> carbonyl hydroperoxide nitrate	(-) 262		
C <sub>5</sub> hydroxy hydroperoxide nitrate	(-) 264		
C <sub>5</sub> dinitrate	(-) 277		
ROOR from INO <sub>2</sub> and HMP and/or CIMS complex btw INP and CH <sub>2</sub> O	(-) 278		
C <sub>5</sub> dihydroperoxide nitrate	(-) 280		
C <sub>5</sub> dinitrooxy epoxide	(-) 293		
ROOR from IHNO <sub>2</sub> and HMP	(-) 294		
ROOR from INO <sub>2</sub> and INO <sub>2</sub>	(-) 377		
ROOR from INO <sub>2</sub> and IHNO <sub>2</sub>	(-) 393		

<sup>A</sup> These sensitivities are dependent on Relative Humidity.

**Table SA2.** List of the general reactions in the kinetic mechanism.

reaction	rate constant <sup>A</sup>	rate source	products source
<b>CH<sub>2</sub>O reactions</b>			
CH <sub>2</sub> O + NO <sub>3</sub> → HNO <sub>3</sub> + HO <sub>2</sub> + CO	$2 \times 10^{-12} \text{ e}^{-2440/T} * (2.5-3.0)$	IUPAC*2.9 <sup>B</sup>	IUPAC <sup>2</sup>
CH <sub>2</sub> O + OH → H <sub>2</sub> O + HO <sub>2</sub> + CO	$5.4 \times 10^{-12} \text{ e}^{135/T}$	IUPAC <sup>2</sup>	IUPAC <sup>2</sup>
HO <sub>2</sub> + CH <sub>2</sub> O → HMP	$9.7 \times 10^{-15} \text{ e}^{625/T}$	IUPAC <sup>2</sup>	IUPAC <sup>2</sup>
HMP → CH <sub>2</sub> O + HO <sub>2</sub>	$2.4 \times 10^{12} \text{ e}^{-7000/T} \text{ s}^{-1}$	IUPAC <sup>2</sup>	IUPAC <sup>2</sup>
HMP + HO <sub>2</sub> → 0.5 (HMHP + O <sub>2</sub> ) + 0.3 (HCOOH + H <sub>2</sub> O + O <sub>2</sub> ) + 0.2 (HCOOH + HO <sub>2</sub> + OH + O <sub>2</sub> )	$5.6 \times 10^{-15} \text{ e}^{2300/T}$	IUPAC <sup>2</sup>	Jenkin et al. <sup>52</sup>
HMP + HMP → HCOOH + CH <sub>2</sub> (OH) <sub>2</sub> + O <sub>2</sub>	$7.0 \times 10^{-13}$	IUPAC <sup>2</sup>	IUPAC <sup>2</sup>

**Table SA2.** List of the general reactions in the kinetic mechanism.

reaction	rate constant <sup>4</sup>	rate source	products source
HMP + HMP → 2 HCOOH + 2HO <sub>2</sub> + O <sub>2</sub>	5.5 x 10 <sup>-12</sup>	IUPAC <sup>2</sup>	IUPAC <sup>2</sup>
HMP + NO → HO <sub>2</sub> + HCOOH + NO <sub>2</sub>	5.6 x 10 <sup>-12</sup>	IUPAC <sup>2</sup>	IUPAC <sup>2</sup>
HMP + NO <sub>3</sub> → HO <sub>2</sub> + HCOOH + NO <sub>2</sub>	1.2 x 10 <sup>-12</sup>	IUPAC <sup>C2</sup>	IUPAC <sup>2</sup>
OH + HCOOH → CO <sub>2</sub> + HO <sub>2</sub> + H <sub>2</sub> O	4.5 x 10 <sup>-13</sup>	IUPAC <sup>2</sup>	IUPAC <sup>2</sup>
HMHP + OH → 0.12 (HMP + H <sub>2</sub> O) + 0.88 (HCOOH + OH + H <sub>2</sub> O)	3.1 x 10 <sup>-11</sup>	Jenkin et al. <sup>52</sup> <sub>D</sub>	Jenkin et al. <sup>52</sup>
CO + OH → HO <sub>2</sub> + CO <sub>2</sub>	k <sub>0</sub> = 5.9 x 10 <sup>-33</sup> (T/300) <sup>-1.4</sup> ; k <sub>∞</sub> = 1.1 x 10 <sup>-12</sup> (T/300) <sup>1.3</sup> ; F <sub>c</sub> = 0.6	JPL <sup>1</sup>	JPL <sup>1</sup>
CO + OH → HO <sub>2</sub> + CO <sub>2</sub>	k <sub>0</sub> = 1.5 x 10 <sup>-13</sup> (T/300) <sup>0.6</sup> ; k <sub>∞</sub> = 2.1 x 10 <sup>-9</sup> (T/300) <sup>6.1</sup> ; F <sub>c</sub> = 0.6	JPL <sup>1</sup>	JPL <sup>1</sup>
<b>HO<sub>x</sub> reactions</b>			
HO <sub>2</sub> + HO <sub>2</sub> → H <sub>2</sub> O <sub>2</sub> + O <sub>2</sub>	(3.0 x 10 <sup>-13</sup> e <sup>460/T</sup> + 2.1 x 10 <sup>-33</sup> e <sup>920/T</sup> M) * (1 + 1.4 x 10 <sup>-21</sup> [H <sub>2</sub> O] e <sup>2200/T</sup> )	JPL <sup>1</sup>	JPL <sup>1</sup>
OH + OH → H <sub>2</sub> O <sub>2</sub>	k <sub>0</sub> = 6.9 x 10 <sup>-31</sup> (T/300) <sup>-1</sup> ; k <sub>∞</sub> = 2.6 x 10 <sup>-11</sup> (T/300) <sup>0</sup> ; F <sub>c</sub> = 0.6	JPL <sup>1</sup>	JPL <sup>1</sup>
OH + OH → H <sub>2</sub> O + O	1.8 x 10 <sup>-12</sup>	JPL <sup>1</sup>	JPL <sup>1</sup>
OH + H <sub>2</sub> O <sub>2</sub> → HO <sub>2</sub> + H <sub>2</sub> O	1.8 x 10 <sup>-12</sup>	JPL <sup>1</sup>	JPL <sup>1</sup>
OH + HO <sub>2</sub> → H <sub>2</sub> O + O <sub>2</sub>	4.8 x 10 <sup>-11</sup> e <sup>250/T</sup>	JPL <sup>1</sup>	JPL <sup>1</sup>
<b>O<sub>3</sub> reactions</b>			
O <sub>3</sub> + HO <sub>2</sub> → OH + 2O <sub>2</sub>	2.03 x 10 <sup>-16</sup> (T/300) <sup>4.57</sup> e <sup>693/T</sup>	IUPAC <sup>3</sup>	IUPAC <sup>3</sup>
O <sub>3</sub> + OH → HO <sub>2</sub> + O <sub>2</sub>	1.7 x 10 <sup>-12</sup> e <sup>-940/T</sup>	JPL <sup>1</sup>	JPL <sup>1</sup>
O( <sup>1</sup> D) + H <sub>2</sub> O → 2OH	1.63 x 10 <sup>-10</sup> e <sup>60/T</sup>	JPL <sup>1</sup>	JPL <sup>1</sup>
O( <sup>1</sup> D) → O	3.3 x 10 <sup>-11</sup> e <sup>55/T</sup> 0.21 M + 2.15 x 10 <sup>-11</sup> e <sup>110/T</sup> 0.78 M s <sup>-1</sup>	JPL <sup>1</sup>	JPL <sup>1</sup>
O + O <sub>3</sub> → 2O <sub>2</sub>	8.0 x 10 <sup>-12</sup> e <sup>-2060/T</sup>	JPL <sup>1</sup>	JPL <sup>1</sup>
O + OH → O <sub>2</sub> + HO <sub>2</sub>	1.8 x 10 <sup>-11</sup> e <sup>180/T</sup>	JPL <sup>1</sup>	JPL <sup>1</sup>
O + HO <sub>2</sub> → OH + O <sub>2</sub>	3.0 x 10 <sup>-11</sup> e <sup>200/T</sup>	JPL <sup>1</sup>	JPL <sup>1</sup>
O + H <sub>2</sub> O <sub>2</sub> → OH + HO <sub>2</sub>	1.4 x 10 <sup>-12</sup> e <sup>-2000/T</sup>	JPL <sup>1</sup>	JPL <sup>1</sup>
O + O <sub>2</sub> → O <sub>3</sub>	6.0 x 10 <sup>-34</sup> (T/300) <sup>-2.4</sup> M	JPL <sup>1</sup>	JPL <sup>1</sup>
<b>NO<sub>x</sub> reactions</b>			
O + NO → NO <sub>2</sub>	k <sub>0</sub> = 9.0 x 10 <sup>-32</sup> (T/300) <sup>-1.5</sup> ; k <sub>∞</sub> = 3.0 x 10 <sup>-11</sup> (T/300) <sup>0</sup> ; F <sub>c</sub> = 0.6	JPL <sup>1</sup>	JPL <sup>1</sup>
O + NO <sub>2</sub> → NO <sub>3</sub>	k <sub>0</sub> = 2.5 x 10 <sup>-31</sup> (T/300) <sup>-1.8</sup> ; k <sub>∞</sub> = 2.2 x 10 <sup>-11</sup> (T/300) <sup>-0.7</sup> ; F <sub>c</sub> = 0.6	JPL <sup>1</sup>	JPL <sup>1</sup>
O + NO <sub>2</sub> → NO + O <sub>2</sub>	5.1 x 10 <sup>-12</sup> e <sup>210/T</sup>	JPL <sup>1</sup>	JPL <sup>1</sup>
O + NO <sub>3</sub> → O <sub>2</sub> + NO <sub>2</sub>	1.0 x 10 <sup>-11</sup>	JPL <sup>1</sup>	JPL <sup>1</sup>
O <sub>3</sub> + NO → O <sub>2</sub> + NO <sub>2</sub>	3 x 10 <sup>-12</sup> e <sup>-1500/T</sup>	JPL <sup>1</sup>	JPL <sup>1</sup>
O <sub>3</sub> + NO <sub>2</sub> → NO <sub>3</sub> + O <sub>2</sub>	1.2 x 10 <sup>-13</sup> e <sup>-2450/T</sup>	JPL <sup>1</sup>	JPL <sup>1</sup>
O <sub>3</sub> + NO <sub>2</sub> → NO + 2O <sub>2</sub>	9.7 x 10 <sup>-19</sup>	Cantrell et al. <sup>5</sup>	Cantrell et al. <sup>5</sup>
NO <sub>2</sub> + NO <sub>3</sub> → NO + NO <sub>2</sub> + O <sub>2</sub>	4.5 x 10 <sup>-14</sup> e <sup>-1260/T</sup>	JPL <sup>1</sup>	JPL <sup>1</sup>



**Table SA2.** List of the general reactions in the kinetic mechanism.

reaction	rate constant <sup>A</sup>	rate source	products source
$\text{NO}_3 + \text{NO}_2 + \text{M} \rightleftharpoons \text{N}_2\text{O}_5 + \text{M}$	$k_0 = 2.0 \times 10^{-30} (T/300)^{-4.4}$ ; $k_\infty = 1.4 \times 10^{-12} (T/300)^{-0.7}$ ; $k_{\text{eq}} = 2.7 \times 10^{-27} e^{11000/T}$ ; $F_c = 0.6$	JPL <sup>1</sup>	JPL <sup>1</sup>
$\text{N}_2\text{O}_5 + \text{H}_2\text{O} + \text{wall} \rightarrow 2\text{HNO}_3$	Varied <sup>E</sup>	NA	Cantrell et al. <sup>5</sup>
$\text{NO}_3 + \text{NO} \rightarrow 2\text{NO}_2$	$1.5 \times 10^{-11} e^{170/T}$	JPL <sup>1</sup>	JPL <sup>1</sup>
$\text{NO}_3 + \text{NO}_3 \rightarrow 2\text{NO}_2 + \text{O}_2$	$8.5 \times 10^{-13} e^{-2450/T}$	JPL <sup>1</sup>	JPL <sup>1</sup>
$\text{NO}_3 + \text{HO}_2 \rightarrow \text{OH} + \text{O}_2 + \text{NO}_2$	$4.0 \times 10^{-12}$	IUPAC <sup>3</sup>	IUPAC <sup>3</sup>
$\text{NO} + \text{HO}_2 \rightarrow \text{NO}_2 + \text{OH}$	$3.3 \times 10^{-12} e^{270/T}$	JPL <sup>1</sup>	JPL <sup>1</sup>
$\text{NO}_2 + \text{HO}_2 \rightarrow \text{HONO} + \text{O}_2$	$5.0 \times 10^{-16}$	JPL <sup>1</sup>	Upper limit in JPL <sup>1</sup>
$\text{NO}_2 + \text{HO}_2 + \text{M} \rightleftharpoons \text{HO}_2\text{NO}_2 + \text{M}$	$k_0 = 2.0 \times 10^{-31} (T/300)^{-3.4}$ ; $k_\infty = 2.9 \times 10^{-12} (T/300)^{-1.1}$ ; $k_{\text{eq}} = 2.1 \times 10^{-27} e^{10900/T}$ ; $F_c = 0.6$	JPL <sup>1</sup>	JPL <sup>1</sup>
$\text{NO} + \text{OH} + \text{M} \rightarrow \text{HONO} + \text{M}$	$k_0 = 7.0 \times 10^{-31} (T/300)^{-2.6}$ ; $k_\infty = 3.6 \times 10^{-11} (T/300)^{-0.1}$ ; $F_c = 0.6$	JPL <sup>1</sup>	JPL <sup>1</sup>
$\text{NO}_2 + \text{OH} + \text{M} \rightarrow \text{HNO}_3 + \text{M}$	$k_0 = 1.8 \times 10^{-30} (T/300)^{-3.0}$ ; $k_\infty = 2.8 \times 10^{-11} (T/300)^0$ ; $F_c = 0.6$	JPL <sup>1</sup>	JPL <sup>1</sup>
$\text{NO}_2 + \text{OH} + \text{M} \rightleftharpoons \text{HOONO} + \text{M}$	$k_0 = 9.1 \times 10^{-32} (T/300)^{-3.9}$ ; $k_\infty = 4.2 \times 10^{-11} (T/300)^{-0.5}$ ; $k_{\text{eq}} = 3.5 \times 10^{-27} e^{10135/T}$ ; $F_c = 0.6$	JPL <sup>1</sup>	JPL <sup>1</sup>
$\text{NO}_3 + \text{OH} \rightarrow \text{NO}_2 + \text{HO}_2$	$2.0 \times 10^{-11}$	IUPAC <sup>3</sup>	IUPAC <sup>3</sup>
$\text{HONO} + \text{OH} \rightarrow \text{NO}_2 + \text{H}_2\text{O}$	$1.8 \times 10^{-11} e^{-390/T}$	JPL <sup>1</sup>	JPL <sup>1</sup>
$\text{HNO}_3 + \text{OH} \rightarrow \text{H}_2\text{O} + \text{NO}_3$	$k_0 = 2.4 \times 10^{-14} e^{460/T}$ ; $k_2 = 2.7 \times 10^{-17} e^{2199/T}$ ; $k_3 = 6.5 \times 10^{-34} e^{1335/T}$ ; $k = k_0 + k_3 \text{M} / (1 + k_3 \text{M} / k_2)$	JPL <sup>1</sup>	JPL <sup>1</sup>
$\text{HO}_2\text{NO}_2 + \text{OH} \rightarrow \text{H}_2\text{O} + \text{O}_2 + \text{NO}_2$	$3.2 \times 10^{-13} e^{690/T}$	IUPAC <sup>3</sup>	IUPAC <sup>3</sup>
$\text{HONO} + \text{HNO}_3 \rightarrow 2\text{NO}_2 + \text{H}_2\text{O}$	$2.71 \times 10^{-17}$	Cantrell et al. <sup>5</sup>	Cantrell et al. <sup>5</sup>

<sup>A</sup> Rate constant units are  $\text{cm}^3 \text{ molec}^{-1} \text{ s}^{-1}$  unless noted otherwise. <sup>B</sup> Increased IUPAC rate constant by a factor such that the experimental results for  $\text{H}_2\text{O}_2$  matched the kinetic mechanism results. <sup>C</sup> Specific rate unknown used IUPAC rate constant/products for  $\text{CH}_3\text{O}_2 + \text{NO}_3$ . <sup>D</sup> Rate constant estimated by Jenkin et al.<sup>52</sup> by SAR method. <sup>E</sup> Varied based on chamber/experiment (see Section 1.1 of the supplementary). See Table S5 for full names of the abbreviations used above.

**Table SA3.** List of isoprene related reactions in the kinetic mechanism.

reaction	rate constant <sup>A</sup>	reaction source	rate constant source
<b>isoprene + OH/O<sub>3</sub> reactions</b>			
$\text{ISOP} + \text{OH} \xrightarrow{\text{O}_2} \text{IHO}_2$	$2.7 \times 10^{-11} e^{390/T}$	MCM v3.2 <sup>4</sup>	IUPAC <sup>2</sup>
$\text{IHO}_2 + \text{NO} \xrightarrow{\text{O}_2} 0.22\text{IHC} + 0.88\text{HO}_2 + 0.39\text{MVK} + 0.27\text{MACR} + 0.66\text{CH}_2\text{O} + 0.88\text{NO}_2 + 0.12\text{ISOPN}$	$2.7 \times 10^{-12} e^{360/T}$	Paulot et al. <sup>53</sup> , MCM v3.2 <sup>4</sup>	MCM v3.2 <sup>4</sup>
$\text{IHO}_2 + \text{NO}_3 \xrightarrow{\text{O}_2} 0.25\text{IHC} + \text{HO}_2 + 0.444\text{MVK} + 0.306\text{MACR} + 0.75\text{CH}_2\text{O} + \text{NO}_2$	$2.3 \times 10^{-12}$	MCM v3.2 <sup>4</sup>	MCM v3.2 <sup>4</sup>

**Table SA3.** List of isoprene related reactions in the kinetic mechanism.

reaction	rate constant <sup>A</sup>	reaction source	rate constant source
$\text{IHO} \xrightarrow{\text{O}_2} 0.45\text{IHC} + 0.55\text{MACR} + 0.55\text{CH}_2\text{O} + \text{HO}_2$	$1.0 \times 10^6 \text{ s}^{-1}$	MCM v3.2 <sup>4</sup>	MCM v3.2 <sup>4</sup>
$\text{IHO}_2 + \text{IHO}_2 \rightarrow 0.18\text{IHC} + 0.22 \text{ MACR} + 0.4\text{IDH} + 1.2 \text{ IHO}$	$2.6 \times 10^{-12}$	MCM v3.2 <sup>4</sup> /Jenkin et al. <sup>54</sup>	Jenkin et al. <sup>30 B</sup>
$\text{IHO}_2 + \text{INO}_2 \rightarrow 0.09\text{IHC} + 0.11\text{MACR} + 0.2\text{IDH} + 0.6\text{IHO} + 0.23\text{INO} + 0.308\text{IHN}\delta + 0.077\text{IHN}\beta + 0.385\text{ICN}$	$3.6 \times 10^{-12}$	MCM v3.2 <sup>4</sup> /Kwan et al. <sup>7</sup> , Jenkin et al. <sup>54</sup> , This work	geometric mean $\text{IHO}_2$ and $\text{INO}_2$ self-reaction
$\text{IHO}_2 + \text{IHNO}_2 \rightarrow 0.09\text{IHC} + 0.11\text{MACR} + 0.2\text{IDH} + 0.6 \text{ IHO} + 0.23\text{IHNO} + 0.385 \text{ IHCN} + 0.385 \text{ IDHN}$	$3.6 \times 10^{-12}$	MCM v3.2 <sup>4</sup> / Kwan et al. <sup>7</sup> , Jenkin et al. <sup>54</sup>	see S2.2
$\text{IPNO}_2 + \text{IHO}_2 \rightarrow 0.23\text{IPNO} + 0.385\text{ICPN} + 0.385\text{IHPN} + 0.6\text{IHO} + 0.09\text{IHC} + 0.11\text{MACR} + 0.2\text{IDH}$	$3.6 \times 10^{-12}$	assume same as $\text{INO}_2 + \text{IHO}_2$	see 2.3
$\text{IHO}_2 + \text{HMP} \rightarrow 0.09\text{IHC} + 0.11\text{MACR} + 0.2\text{IDH} + 0.6\text{IHO} + \text{HCOOH} + \text{HO}_2$	$3.8 \times 10^{-12}$	MCM v3.2 <sup>4</sup> /IUPAC <sup>2</sup> /Jenkin et al. <sup>54</sup>	geometric mean HMP and $\text{IHO}_2$ self-reaction
$\text{IHO}_2 + \text{HO}_2 \rightarrow 0.937\text{ISOPOOH} + 0.063\text{OH} + 0.025\text{MACR} + 0.038\text{MVK} + 0.063\text{HO}_2 + 0.063 \text{ CH}_2\text{O}$	$2.91 \times 10^{-13} \text{ e}^{1300/T} * 0.706$	Liu et al. <sup>55</sup>	Saunders et al. <sup>4</sup>
$\text{ISOPOOH} + \text{OH} \rightarrow 0.7\text{IO}_2 + 0.3\text{IHC} + 0.3 \text{ OH}$	$3.8 \times 10^{-12} \text{ e}^{200/T}$	Paulot et al. <sup>34</sup>	Paulot et al. <sup>34</sup>
$\text{ISOPOOH} + \text{OH} \rightarrow \text{IEPOX} + \text{OH}$	$1.9 \times 10^{-11} \text{ e}^{390/T}$	Paulot et al. <sup>34</sup>	Paulot et al. <sup>34</sup>
$\text{IEPOX} + \text{OH} \rightarrow 0.07\text{GLYC} + 0.09\text{HACET} + \text{Products}$	$1.15 \times 10^{-11}$	Bates et al. <sup>27</sup> , (high NO yields)	Bates et al. <sup>27 C</sup>
$\text{ISOP} + \text{O}_3 \rightarrow 0.41\text{MACR} + 0.16\text{MVK} + 0.26\text{OH} + 0.26\text{HO}_2 + \text{Products}$	$1.03 \times 10^{-14} \text{ e}^{-1995/T}$	see notes <sup>D</sup>	IUPAC <sup>2</sup>
$\text{IHC} + \text{OH} \xrightarrow{\text{O}_2} \xrightarrow{\text{NO}, -\text{NO}_2} \text{HO}_2 + 0.59\text{HACET} + 0.59\text{GLYX} + 0.41\text{MGLYX} + 0.41\text{GLYC}$	$4.52 \times 10^{-11}$	MCM v3.2 <sup>4</sup> (include only main products)	MCM v3.2 <sup>4</sup>
$\text{IDH} + \text{OH} \xrightarrow{\text{O}_2} \text{IHC} + \text{HO}_2$	$9.3 \times 10^{-11}$	MCM v3.2 <sup>4</sup>	MCM v3.2 <sup>4</sup>
<b>NO<sub>2</sub> reactions (included as verification that high [NO<sub>2</sub>] has only a minor impact on the chemistry)</b>			
$\text{ISOP} + \text{NO}_2 \rightarrow \text{Products}$	$1.10 \times 10^{-19}$	Bernard et al. <sup>56</sup>	Bernard et al. <sup>56</sup>
$\text{INO} + \text{NO}_2 \rightarrow \text{INO}_3\text{N}$	$2.8 \times 10^{-11}$	IUPAC <sup>2</sup>	IUPAC <sup>2 E</sup>
$\text{INO}_2 + \text{NO}_2 + \text{M} \rightarrow \text{INO}_4\text{N}$	$k_0 = 1.3 \times 10^{-29} (\text{T}/300)^{-6.2}$ , $k_\infty = 8.8 \times 10^{-12}$ , $F_c = 0.31$	IUPAC <sup>2</sup>	IUPAC <sup>2 F</sup>
$\text{INO}_4\text{N} + \text{M} \rightarrow \text{INO}_2 + \text{NO}_2 + \text{M}$	$k_0 = 4.8 \times 10^{-4} \text{ e}^{-9285/T}$ , $k_\infty = 8.8 \times 10^{-15} \text{ e}^{-10440/T}$ , $F_c = 0.31$	IUPAC <sup>2</sup>	IUPAC <sup>2 G</sup>
$\text{IN}^* + \text{NO}_2 \rightarrow \text{INO}_2\text{N}$	$2.37 \times 10^{-12}$	Canosa et al. <sup>57</sup>	Canosa et al. <sup>57 H</sup>
<b>Isoprene + NO<sub>3</sub> (first generation) reactions</b>			
$\text{ISOP} + \text{NO}_3 \rightarrow \text{IN}^*$	$3.15 \times 10^{-12} \text{ e}^{-450/T}$	IUPAC <sup>2</sup>	IUPAC <sup>2</sup>

**Table SA3.** List of isoprene related reactions in the kinetic mechanism.

reaction	rate constant <i>A</i>	reaction source	rate constant source
$\text{IN}^\bullet + \text{O}_2 \rightarrow \text{INO}_2$	$k_0 = 5.9 \times 10^{-29}$ $(\text{T}/300)^{-3.8}; k_{\infty}$ $= 7.8 \times 10^{-12};$ $F_e = 0.54$	IUPAC <sup>2</sup>	IUPAC <sup>2</sup>
$\text{INO}_2 + \text{HO}_2 \rightarrow 0.22\text{MVK} + 0.015\text{MACR}$ $+ 0.235\text{OH} + 0.235\text{NO}_2 + 0.235\text{CH}_2\text{O}$ $+ 0.54\text{INP}\delta + 0.23\text{INP}\beta$	$2.91 \times 10^{-13}$ $e^{1300/\text{T}} * 0.706$	see Section 4.2 of main text.	Saunders et al. <sup>4</sup>
$\text{INO}_2 + \text{INO}_2 \rightarrow 0.39\text{INO} + 0.67\text{ICN}$ $+ 0.10\text{MACR} + 0.616\text{IHN}\delta + 0.154\text{IHN}\beta$ $+ 0.035\text{INO}_2\text{IN}$	$5.0 \times 10^{-12}$	see S1.2, Section 4.3	see Section 4.3 of main text.
$\text{INO}_2 + \text{MHP} \rightarrow 0.195\text{INO} + 0.34\text{ICN}$ $+ 0.05\text{MACR} + 0.308\text{IHN}\delta + 0.077\text{IHN}\beta$ $+ 0.965\text{HO}_2 + 0.965\text{HCOOH}$ $+ 0.035\text{INO}_2\text{HM}$	$5.2 \times 10^{-12}$	IUPAC <sup>2</sup> /See S1.2, Section 4.3	geometric mean of $\text{INO}_2$ and HMP self-reaction
$\text{INO}_2 + \text{NO}_3 \rightarrow 0.42\text{MVK} + 0.04 \text{MACR}$ $+ 0.46\text{CH}_2\text{O} + 1.46\text{NO}_2 + 0.54\text{ICN}$ $+ 0.54\text{HO}_2$	$2.3 \times 10^{-12}$	MCM v3.2 <sup>4</sup> , Section 4.1	MCM v3.2 <sup>4</sup>
$\text{INO}_2 + \text{NO} \rightarrow 0.12\text{IDN} + 0.47\text{ICN} + 0.47\text{HO}_2$ $+ 1.29\text{NO}_2 + 0.37\text{MVK} + 0.04\text{MACR}$ $+ 0.41\text{CH}_2\text{O}$	$2.7 \times 10^{-12} e^{360/\text{T}}$	assumed same as $\text{IHO}_2 + \text{NO}$ , Section 4.1	MCM v3.2 <sup>4</sup>
$\text{INO} + \text{O}_2 \rightarrow 0.88\text{ICN} + 0.88\text{HO}_2$ $+ 0.12\text{MACR} + 0.12\text{CH}_2\text{O} + 0.12\text{NO}_2$	$2.5 \times 10^{-14} e^{-300/\text{T}}$	MCM v3.2 <sup>4</sup> , Section 4.3	MCM v3.2 <sup>4</sup>
<b>[1,5]-H-Shift of trans-[1,4]-INO reactions</b>			
$\text{INO} \xrightarrow{\text{O}_2} \text{IHNO}_2$	$2 \times 10^5 \text{ s}^{-1}$	Kwan et al. <sup>7</sup>	see S2.2
$\text{IHNO}_2 + \text{NO}_3 \rightarrow \text{IHNO} + \text{NO}_2$	$2.3 \times 10^{-12}$	assume same as $\text{INO}_2 + \text{NO}_3$	assume same as $\text{INO}_2 +$ $\text{NO}_3$
$\text{IHNO}_2 + \text{NO} \rightarrow \text{IHNO} + \text{NO}_2$	$2.7 \times 10^{-12} e^{360/\text{T}}$	assume same as $\text{INO}_2 + \text{NO}$	assume same as $\text{INO}_2 +$ $\text{NO}$
$\text{IHNO} + \text{O}_2 \rightarrow \text{IHCN} + \text{HO}_2$	$2.5 \times 10^{-14} e^{-300/\text{T}}$	assume same as $\text{INO} + \text{O}_2$	assume same as $\text{INO} +$ $\text{O}_2$
$\text{IHNO}_2 + \text{HO}_2 \rightarrow \text{IHPN}$	$2.91 \times 10^{-13} e^{1300/\text{T}} * 0.706$	assume IHPN only product	Saunders et al. <sup>4</sup>
$\text{IHNO}_2 + \text{IHNO}_2 \rightarrow 0.46\text{IHNO}$ $+ 0.77\text{IHCN} + 0.77\text{IDHN}$	$2 * 5.0 \times 10^{-12}$	assume same as $\text{INO}_2 + \text{INO}_2$	see S2.2
$\text{IHNO}_2 + \text{INO}_2 \rightarrow 0.195\text{INO} + 0.385\text{ICN}$ $+ 0.308\text{IHN}\delta + 0.077\text{IHN}\beta + 0.385\text{IHCN}$ $+ 0.385\text{IDHN} + 0.035\text{INO}_2\text{IHN}$ $+ 0.195\text{IHNO}$	$2 * 5.0 \times 10^{-12}$	assume same as $\text{INO}_2 + \text{INO}_2$	see S2.2
$\text{IHNO}_2 + \text{HMP} \rightarrow 0.195\text{IHNO}$ $+ 0.385\text{IHCN} + 0.385\text{IDHN} + 0.965\text{HO}_2$ $+ 0.965\text{HCOOH} + 0.035\text{IHNO}_2\text{HM}$	$2 * 5.2 \times 10^{-12}$	assume same as $\text{INO}_2 + \text{HMP}$	see S2.2
<b>[1,6]-H shift of trans-[1,4]-INO<sub>2</sub> reactions</b>			
$\text{INO}_2 \xrightarrow{\text{O}_2} \text{IPNO}_2$	$4 \times 10^{-4} \text{ s}^{-1}$	see S2.3	see S2.3
$\text{IPNO}_2 \xrightarrow{1,4\text{-H shift}} \text{ICPN} + \text{OH}$	$2 \times 10^{-2} \text{ s}^{-1}$	see S2.3	see S2.3
$\text{IPNO}_2 + \text{NO} \rightarrow \text{IPNO} + \text{NO}_2$	$2.7 \times 10^{-12} e^{360/\text{T}}$	assume same as $\text{INO}_2 + \text{NO}$	assume same as $\text{INO}_2 +$ $\text{NO}$
$\text{IPNO}_2 + \text{NO}_3 \rightarrow \text{IPNO} + \text{NO}_2$	$2.3 \times 10^{-12}$	assume same as $\text{INO}_2 + \text{NO}_3$	assume same as $\text{INO}_2 +$ $\text{NO}_3$

**Table SA3.** List of isoprene related reactions in the kinetic mechanism.

reaction	rate constant <i>A</i>	reaction source	rate constant source
IPNO + O <sub>2</sub> → ICPN + HO <sub>2</sub>	$2.5 \times 10^{-14} e^{-300/T}$	assume same as INO + O <sub>2</sub>	assume same as INO + O <sub>2</sub>
IPNO <sub>2</sub> + HO <sub>2</sub> → IDPN	$2.91 \times 10^{-13} e^{1300/T} * 0.706$	assumed same as IHNO <sub>2</sub> + HO <sub>2</sub>	Saunders et al. <sup>4</sup>
IPNO <sub>2</sub> + IPNO <sub>2</sub> → 0.46IPNO + 0.77ICPN + 0.77IHPN	$2 * 5.0 \times 10^{-12}$	assume same as INO <sub>2</sub> + INO <sub>2</sub>	See S2.3
IPNO <sub>2</sub> + INO <sub>2</sub> → 0.23IPNO + 0.385ICPN + 0.385IHPN + 0.23INO + 0.308IHNδ + 0.077IHNβ + 0.385ICN	$2 * 5.0 \times 10^{-12}$	assume same as INO <sub>2</sub> + INO <sub>2</sub>	see S2.3
IPNO <sub>2</sub> + HMP → 0.23IPNO + 0.385ICPN + 0.385IHPN + HCOOH + HO <sub>2</sub>	$2 * 5.2 \times 10^{-12}$	assume same as INO <sub>2</sub> + MHP	see 2.3
IPNO <sub>2</sub> + IHNO <sub>2</sub> → 0.23IPNO + 0.385ICPN + 0.385IHPN + 0.23IHNO + 0.385IDHN + 0.385IHCN	$2 * 5.0 \times 10^{-12}$	assume same as INO <sub>2</sub> + INO <sub>2</sub>	see S2.2/S2.3
<b>INP reactions</b>			
INPδ + wall → Products	$9 \times 10^{-6} \text{ s}^{-1}$	NA	this work, see S1.3
INPβ + wall → Products	$9 \times 10^{-6} \text{ s}^{-1}$	NA	this work, see S1.3
INHEβ + wall → Products	$9 \times 10^{-6} \text{ s}^{-1}$	NA	this work, see S1.3
INHEδ + wall → Products	$9 \times 10^{-6} \text{ s}^{-1}$	NA	this work, see S1.3
INHEδ2 + wall → Products	$9 \times 10^{-6} \text{ s}^{-1}$	NA	this work, see S1.3
INPδ + OH → 0.37INHEδ + 0.37OH + 0.08IHPE + 0.08NO <sub>2</sub> + 0.55INPHO <sub>2</sub> δ	$1.1 \times 10^{-10}$	see S1.4	Lee et al. <sup>6 *</sup>
INPδ + OH → INO <sub>2</sub> + HO <sub>2</sub>	$6.9 \times 10^{-12}$	see S1.4	estimated from St. Clair et al. <sup>9</sup>
INPβ + OH → 0.78INHEβ + 0.78OH + 0.22INPHO <sub>2</sub> β	$4.2 \times 10^{-11}$	see S1.4	Lee et al. <sup>6 *</sup>
INPβ + OH → INO <sub>2</sub> + HO <sub>2</sub>	$6.9 \times 10^{-12}$	see S1.4	estimated from St. Clair et al. <sup>9</sup>
INPHO <sub>2</sub> β + HO <sub>2</sub> → 0.27IHDPN + 0.73OH + 0.73HO <sub>2</sub> + 0.73CH <sub>2</sub> O + 0.72C4CPN_A + 0.01C4CPN_K	$2.91 \times 10^{-13} e^{1300/T} * 0.706$	see S1.4	Saunders et al. <sup>4</sup>
INPHO <sub>2</sub> β + NO <sub>3</sub> → NO <sub>2</sub> + HO <sub>2</sub> + CH <sub>2</sub> O + 0.98C4CPN_A + 0.02C4CPN_K	$2.3 \times 10^{-12}$	see S1.4	assume same as INO <sub>2</sub> + NO <sub>3</sub>
INPHO <sub>2</sub> β + NO → 0.04IHPDN + 0.96NO <sub>2</sub> + 0.96HO <sub>2</sub> + 0.02C4CPN_K + 0.94C4CPN_A + 0.96CH <sub>2</sub> O	$2.7 \times 10^{-12} e^{360/T}$	see S1.4	assume same as INO <sub>2</sub> + NO
INPHO <sub>2</sub> δ + HO <sub>2</sub> → 0.27IHDPN + 0.06ETHLN + 0.73OH + 0.73HO <sub>2</sub> + 0.67PROPNN + 0.67HPETHNL + 0.06HPAC	$2.91 \times 10^{-13} e^{1300/T} * 0.706$	see S1.4	Saunders et al. <sup>4</sup>
INPHO <sub>2</sub> δ + NO <sub>3</sub> → HO <sub>2</sub> + NO <sub>2</sub> + 0.92PROPNN + 0.92HPETHNL + 0.08HPAC + 0.08ETHLN	$2.3 \times 10^{-12}$	see S1.4	assume same as INO <sub>2</sub> + NO <sub>3</sub>
INPHO <sub>2</sub> δ + NO → 0.04IHPDN + 0.96HO <sub>2</sub> + 0.96NO <sub>2</sub> + 0.88PROPNN + 0.08ETHLN + 0.88HPETHNL + 0.08HPAC	$2.7 \times 10^{-12} e^{360/T}$	see S1.4	assume same as INO <sub>2</sub> + NO

**Table SA3.** List of isoprene related reactions in the kinetic mechanism.

reaction	rate constant <sub>A</sub>	reaction source	rate constant source
INHEδ + OH → 0.1INCE + 0.27HACET + 0.73CO + 0.27NO <sub>2</sub> + 0.27CH <sub>2</sub> O + 0.17PROPNN + 0.17GLYX + 0.46C4CHN_A	8.4 x 10 <sup>-12</sup>	see S1.4	assumed same as δ-IEPOX, Bates et al. <sup>27</sup>
INHEβ + OH → 0.08INCE + 0.31GLYC + 0.43NO <sub>2</sub> + 0.31MGLYX + 0.20PROPNN + 0.20GLYX + 0.12C4DCH + 0.41CH <sub>2</sub> O + 0.26C4CHN_A + 0.02C4DCN + 0.01HACET + 0.01ETHLN	1.25 x 10 <sup>-11</sup>	see S1.4	assumed same as β-IEPOX (avg between cis and trans) <sup>27</sup>
INHEδ2 + OH → 0.1INCE + 0.9MGLYX + 0.9GLYC + 0.9NO <sub>2</sub>	8.4 x 10 <sup>-12</sup>	see S1.4	assumed same as INHEδ + OH
INPδ + NO <sub>3</sub> → 0.35IDNE + 0.35OH + 0.11INPE + 0.11NO <sub>2</sub> + Products	5 x 10 <sup>-15</sup>	Kwan et al. <sup>7</sup>	see S1.3
INPβ + NO <sub>3</sub> → 0.35IDNE + 0.35OH + Products	5 x 10 <sup>-15</sup>	Kwan et al. <sup>7</sup>	see S1.3
INPδ + O <sub>3</sub> → 0.2OH + 0.17C3CNO <sub>2</sub> + 0.03C3CPO <sub>2</sub> + 0.67PROPNN + 0.13HPAC + 0.84HPETHNL + 0.16ETHLN	1.3 x 10 <sup>-17</sup>	see S1.4 <sup>I</sup>	see S1.3
INPβ + O <sub>3</sub> → Products	3.8 x 10 <sup>-19</sup>	NA	Lee et al. <sup>6 *</sup>
<b>ICN reactions</b>			
ICN + wall → Products	6 x 10 <sup>-6</sup> s <sup>-1</sup>	NA	this work, see S1.3
ICN + OH $\xrightarrow{O_2}$ 0.51ICHNO <sub>2</sub> I5 + 0.08NO <sub>2</sub> + 0.41ICHNO <sub>2</sub> I4 + 0.08ICHE	1.1 x 10 <sup>-10</sup>	see S1.4	Lee et al. <sup>6 *</sup>
ICN + OH $\xrightarrow{\text{H-abstraction}}$ Products	2.0 x 10 <sup>-11</sup>	NA	MCM v3.2 <sup>4</sup>
ICHNO <sub>2</sub> I5 → 0.86C4CPN_A + CO + HO <sub>2</sub> + 0.14C4CPN_K	> 0.5 s <sup>-1</sup>	see S1.4	assumed > [1,4]-H shift in <sup>19</sup>
ICHNO <sub>2</sub> I4 → 0.56C4CHN_A + 0.44C4CHN_K + OH + CO	0.5 s <sup>-1</sup>	see S1.4	assumed same as [1,4]-H shift in <sup>19</sup>
ICHNO <sub>2</sub> I4 + HO <sub>2</sub> → 0.27ICHPN + 0.73OH + 0.73HO <sub>2</sub> + 0.32PROPNN + 0.32GLYX + 0.25MGLYX + 0.25ETHLN + 0.08C4CHN_A + 0.07C4CHN_K + 0.15CO	2.91 x 10 <sup>-13</sup> e <sup>1300/T</sup> * 0.706	see S1.4	Saunders et al. <sup>4</sup>
ICHNO <sub>2</sub> I4 + NO <sub>3</sub> → NO <sub>2</sub> + 0.44PROPNN + 0.44GLYX + 0.21CO + 0.35 MGLYX + 0.35ETHLN + HO <sub>2</sub> + 0.12C4CHN_A + 0.09C4CHN_K	2.3 x 10 <sup>-12</sup>	see S1.4	assume same as INO <sub>2</sub> + NO <sub>3</sub>
ICHNO <sub>2</sub> I4 + NO → 0.04IHCDN + 0.96NO <sub>2</sub> + 0.96HO <sub>2</sub> + 0.43PROPNN + 0.43GLYX + 0.34MGLYX + 0.34ETHLN + 0.11C4CHN_A + 0.09C4CHN_K + 0.2CO	2.7 x 10 <sup>-12</sup> e <sup>360/T</sup>	see S1.4	assume same as INO <sub>2</sub> + NO
ICN + NO <sub>3</sub> → 0.1INCE + 0.1NO <sub>2</sub> + Products	8.1 x 10 <sup>-15</sup>	see S3	assumed same as INP + NO <sub>3</sub>
ICN + O <sub>3</sub> → 0.2OH + 0.15C3CNO <sub>2</sub> + 0.05C3DCO <sub>2</sub> + 0.59PROPNN + 0.21MGLYX + 0.74GLYX + 0.26ETHLN	3.2 x 10 <sup>-18</sup>	see S1.4 <sup>J</sup>	see S1.3

**Table SA3.** List of isoprene related reactions in the kinetic mechanism.

reaction	rate constant <sub>A</sub>	reaction source	rate constant source
<b>IHN reactions</b>			
IHNδ + wall → Products	$7 \times 10^{-6} \text{ s}^{-1}$	NA	this work, see S1.3
IHNβ + wall → Products	$7 \times 10^{-6} \text{ s}^{-1}$	NA	this work, see S1.3
IHNδ + OH → 0.92IDHNO <sub>2</sub> δ + 0.08IEPOX + 0.08NO <sub>2</sub>	$1.1 \times 10^{-10}$	see S1.4	Lee et al. <sup>6</sup> *
IHNβ + OH → IDHNO <sub>2</sub> β	$4.2 \times 10^{-11}$	see S1.4	Lee et al. <sup>6</sup> *
IDHNO <sub>2</sub> δ + HO <sub>2</sub> → 0.27IDHPN + 0.73OH + 0.73HO <sub>2</sub> + 0.09HACET + 0.09ETHLN + 0.58PROPNN + 0.58GLYC + 0.04C4CHN_A + 0.02C4CHN_K + 0.06CH <sub>2</sub> O	$2.91 \times 10^{-13} \text{ e}^{1300/T} * 0.706$	see S1.4	Saunders et al. <sup>4</sup>
IDHNO <sub>2</sub> δ + NO → 0.04IDHDN + 0.96HO <sub>2</sub> + 0.96NO <sub>2</sub> + 0.12HACET + 0.12ETHLN + 0.77PROPNN + 0.77GLYC + 0.06C4CHN_A + 0.02C4CHN_K + 0.08CH <sub>2</sub> O	$2.7 \times 10^{-12} \text{ e}^{360/T}$	see S1.4	assume same as INO <sub>2</sub> + NO
IDHNO <sub>2</sub> δ + NO <sub>3</sub> → HO <sub>2</sub> + NO <sub>2</sub> + 0.12HACET + 0.12ETHLN + 0.80GLYC + 0.80PROPNN + 0.06C4CHN_A + 0.02C4CHN_K + 0.08CH <sub>2</sub> O	$2.3 \times 10^{-12}$	see S1.4	assume same as INO <sub>2</sub> + NO <sub>3</sub>
IDHNO <sub>2</sub> β + HO <sub>2</sub> → 0.27IDHPN + 0.73OH + 0.73HO <sub>2</sub> + 0.56HACET + 0.17CH <sub>2</sub> O + 0.56ETHLN + 0.17C4CHN_K	$2.91 \times 10^{-13} \text{ e}^{1300/T} * 0.706$	see S1.4	Saunders et al. 2003
IDHNO <sub>2</sub> β + NO → 0.04IDHDN + 0.96HO <sub>2</sub> + 0.96NO <sub>2</sub> + 0.74HACET + 0.74ETHLN + 0.23C4CHN_K + 0.23 CH <sub>2</sub> O	$2.7 \times 10^{-12} \text{ e}^{360/T}$	see S1.4	assume same as INO <sub>2</sub> + NO
IDHNO <sub>2</sub> β + NO <sub>3</sub> → HO <sub>2</sub> + NO <sub>2</sub> + 0.76HACET + 0.76ETHLN + 0.23C4CHN_K + 0.23CH <sub>2</sub> O	$2.3 \times 10^{-12}$	see S1.4	assume same as INO <sub>2</sub> + NO <sub>3</sub>
IHNδ + NO <sub>3</sub> → 0.11INHEδ2 + 0.11NO <sub>2</sub> + Products	$7 \times 10^{-14}$	see S3	Rollins et al. <sup>13</sup>
IHNβ + NO <sub>3</sub> → Products	$7 \times 10^{-14}$	see S3	Rollins et al. <sup>13</sup>
IHNδ + O <sub>3</sub> → 0.2OH + 0.17C3CNO <sub>2</sub> + 0.03C3CHO <sub>2</sub> + 0.69PROPNN + 0.11HACET + 0.86GLYC + 0.14ETHLN	$2.8 \times 10^{-17}$	see S1.4 <sup>K</sup>	Lee et al. <sup>6</sup> *
IHNβ + O <sub>3</sub> → Products	$3.8 \times 10^{-19}$	NA	Lee et al. <sup>6</sup> *
<b>MACR reactions</b>			
MACR + O <sub>3</sub> → Products	$1.4 \times 10^{-15} \text{ e}^{-2100/T}$	NA	MCM v3.2 <sup>4</sup>
MACR + OH → 0.45MACRO <sub>2</sub> + 0.55MACRHO <sub>2</sub>	$8.0 \times 10^{-12} \text{ e}^{380/T}$	Orlando et al. <sup>58</sup>	MCM v3.2 <sup>4</sup> /IUPAC <sup>2</sup>
MACRO <sub>2</sub> + HO <sub>2</sub> → 0.4MPAA + 0.4CO <sub>2</sub> + 0.4OH + 0.4PENYLO <sub>2</sub> + 0.2MAA + 0.2O <sub>3</sub>	$5.2 \times 10^{-13} \text{ e}^{980/T}$	assumed similar to acetylperoxy + HO <sub>2</sub> <sup>59 L</sup>	assumed similar to acetylperoxy + HO <sub>2</sub> , IUPAC <sup>2</sup>
MACRO <sub>2</sub> + NO → 0.03C4CN + 0.967CO <sub>2</sub> + 0.96PENYLO <sub>2</sub> + NO <sub>2</sub>	$8.7 \times 10^{-12} \text{ e}^{290/T}$	MCM v3.2 <sup>4 M</sup>	MCM v3.2 <sup>4</sup>

**Table SA3.** List of isoprene related reactions in the kinetic mechanism.

reaction	rate constant <sub>A</sub>	reaction source	rate constant source
MACRO <sub>2</sub> + NO <sub>3</sub> → CO <sub>2</sub> + PENYLO <sub>2</sub> + NO <sub>2</sub>	2.3 x 10 <sup>-12</sup> *1.74	MCM v3.2 <sup>4,N</sup>	MCM v3.2 <sup>4</sup>
MACRHO <sub>2</sub> $\xrightarrow{[1,4]\text{-H shift}}$ HACET + CO + OH	0.5 s <sup>-1</sup>	Crounse et al. <sup>19</sup>	Crounse et al. <sup>19</sup>
MACRHO <sub>2</sub> + HO <sub>2</sub> → 0.42C4CHP + 0.58OH + 0.58HACET + 0.58CO + 0.58HO <sub>2</sub>	2.91 x 10 <sup>-13</sup> e <sup>1300/T</sup> *0.625	assumed similar to CH <sub>3</sub> C(O)CH(O <sub>2</sub> )CH <sub>3</sub> + HO <sub>2</sub> <sup>60</sup>	Saunders et al. <sup>4</sup>
MACRHO <sub>2</sub> + NO → 0.03C4CHN + 0.97NO <sub>2</sub> + 0.97HACET + 0.97CO + 0.97 HO <sub>2</sub>	2.7 x 10 <sup>-12</sup> e <sup>360/T</sup>	Crounse et al. <sup>19,O</sup>	MCM v3.2 <sup>4</sup>
MACRHO <sub>2</sub> + NO <sub>3</sub> → NO <sub>2</sub> + HACET + CO + HO <sub>2</sub>	2.3 x 10 <sup>-12</sup>	estimated from MACRHO <sub>2</sub> + NO	MCM v3.2 <sup>4</sup>
<b>MVK reactions</b>			
MVK + OH → MVKHO <sub>2</sub>	2.6 x 10 <sup>-12</sup> e <sup>610/T</sup>	MCM v3.2 <sup>4</sup>	MCM v3.2 <sup>4</sup>
MVK + O <sub>3</sub> → Products	8.5 x 10 <sup>-16</sup> e <sup>-1520/T</sup>	NA	MCM v3.2 <sup>4</sup>
MVKHO <sub>2</sub> + HO <sub>2</sub> → 0.04MGLYX + 0.18HO <sub>2</sub> + 0.36GLYC + 0.36C2CO <sub>2</sub> + 0.04CH <sub>2</sub> O + 0.54OH + 0.46C4CHP + 0.14C4DCH	2.91 x 10 <sup>-13</sup> e <sup>1300/T</sup> *0.625	Praske et al. <sup>18,P</sup>	Saunders et al. <sup>4</sup>
MVKHO <sub>2</sub> + NO → 0.04C4CHN + 0.74GLYC + 0.74C2CO <sub>2</sub> + 0.96NO <sub>2</sub> + 0.22CH <sub>2</sub> O + 0.22MGLYX + 0.22HO <sub>2</sub>	2.7 x 10 <sup>-12</sup> e <sup>360/T</sup>	Praske et al. <sup>18</sup>	assume same as INO <sub>2</sub> + NO
MVKHO <sub>2</sub> + NO <sub>3</sub> → 0.76GLYC + 0.76C2CO <sub>2</sub> + NO <sub>2</sub> + 0.24CH <sub>2</sub> O + 0.24MGLYX + 0.24HO <sub>2</sub>	2.3 x 10 <sup>-12</sup>	estimated from MVKHO <sub>2</sub> + NO	assume same as INO <sub>2</sub> + NO <sub>3</sub>
<b>miscellaneous reactions</b>			
GLYC + OH → Products	1.1 x 10 <sup>-11</sup>	NA	JPL <sup>1</sup>
HPETHNL + OH → Products	1.1 x 10 <sup>-11</sup>	NA	assume similar to GLYC + OH
PROPNN + OH → MGLYX + NO <sub>2</sub>	1.0 x 10 <sup>-12</sup>	MCM v3.2 <sup>4</sup>	MCM v3.2 <sup>4</sup>
ETHLN + OH → Products	3.4 x 10 <sup>-12</sup>	NA	MCM v3.2 <sup>4</sup>
IHCN + OH → Products	1 x 10 <sup>-11</sup>	NA	match expt decay
IHPN + OH → Products	1 x 10 <sup>-11</sup>	NA	match expt decay
IDHN + OH → Products	1 x 10 <sup>-11</sup>	NA	match expt decay
C4CHN_A + OH → PROPNN + HO <sub>2</sub> + CO	1.7 x 10 <sup>-11</sup>	assume H abstracted from carbonyl	Kwok and Atkinson <sup>10</sup>
C4CPN_A + OH → PROPNN + OH + CO	1.7 x 10 <sup>-11</sup>	assume H abstracted from carbonyl	Kwok and Atkinson <sup>10</sup>
<b>reactions included to test different decomposition branching ratios for ICHNO<sub>2</sub>I4 (Section S1.4)<sup>Q</sup></b>			
ICHNO <sub>2</sub> I4 + HO <sub>2</sub> → 0.27ICHPN + 0.73OH + 0.73HO <sub>2</sub> + 0.41C4CHN_A + 0.32C4CHN_K + 0.73CO	2.91 x 10 <sup>-13</sup> e <sup>1300/T</sup> *0.706	see S1.4	Saunders et al. <sup>4</sup>
ICHNO <sub>2</sub> I4 + NO <sub>3</sub> → NO <sub>2</sub> + HO <sub>2</sub> + 0.56C4CHN_A + 0.44C4CHN_K + CO	2.3 x 10 <sup>-12</sup>	see S1.4	assume same as INO <sub>2</sub> + NO <sub>3</sub>

**Table SA3.** List of isoprene related reactions in the kinetic mechanism.

reaction	rate constant <sup>A</sup>	reaction source	rate constant source
ICHNO <sub>2</sub> I4 + NO → 0.04IHCDN + 0.96NO <sub>2</sub> + 0.96HO <sub>2</sub> + 0.54C4CHN_A + 0.42C4CHN_K + 0.96CO	2.7 x 10 <sup>-12</sup> e <sub>360/T</sub>	see S1.4	assume same as INO <sub>2</sub> + NO
<b>reactions included to test reduced INHE yield from INP + OH (Section 4.4.1)<sup>Q</sup></b>			
INPδ + OH → 0.24INHEδ + 0.24OH + 0.08IHPE + 0.08NO <sub>2</sub> + 0.68INPHO <sub>2</sub> δ	1.1 x 10 <sup>-10</sup>	Section 4.4.1	Lee et al. <sup>6 *</sup>
INPβ + OH → 0.50INHEβ + 0.50OH + 0.50INPHO <sub>2</sub> β	4.2 x 10 <sup>-11</sup>	Section 4.4.1	Lee et al. <sup>6 *</sup>

\* Because actual rate constant is unknown assumed OH rate constant is the same as the OH rate constant for hydroxynitrates produced from high NO<sub>x</sub> OH isoprene oxidation. \*\* Branching ratios only estimated to verify probability of chemistry occurring through this pathway. Branching ratios need to be experimentally verified with synthetic standards. <sup>A</sup> Rate constant units are in cm<sup>3</sup> molec<sup>-1</sup> s<sup>-1</sup> unless noted otherwise. <sup>B</sup> Rate constant calculated using a weighted average of the distribution fractions and the rate constants for all the IHO<sub>2</sub> isomers reported by Jenkin et al. 1998. <sup>C</sup> Calculated assuming cis: trans β-IEPOX ratio is 1:2.13 and no δ-IEPOX forms. <sup>D</sup> MVK/MACR<sup>61-62</sup>; OH<sup>63-65</sup>; HO<sub>2</sub><sup>66</sup>. <sup>E</sup> Based on C<sub>2</sub>H<sub>5</sub>O + NO<sub>2</sub> rate constant. <sup>F</sup> Based on C<sub>2</sub>H<sub>5</sub>O<sub>2</sub> + NO<sub>2</sub> rate constant. <sup>G</sup> Based on C<sub>2</sub>H<sub>5</sub>O<sub>2</sub>NO<sub>2</sub> decomposition rate constant. <sup>H</sup> Based on CH<sub>3</sub> + NO<sub>2</sub> rate constant. <sup>I</sup> Products for C3CNO<sub>2</sub> and C3CPO<sub>2</sub> were not included in the kinetic mechanism. <sup>J</sup> Products for C3CNO<sub>2</sub> and C3DCO<sub>2</sub> were not included in the kinetic mechanism. <sup>K</sup> Products for C3CNO<sub>2</sub> and C3CHO<sub>2</sub> were not included in the kinetic mechanism. <sup>L</sup> Products for PENYLO<sub>2</sub> were not included in the kinetic mechanism. <sup>M</sup> Nitrate yield from secondary RO<sub>2</sub> of MVK<sup>18</sup>. <sup>N</sup> Products for PENYLO<sub>2</sub> were not included in the kinetic mechanism. <sup>O</sup> Assume nitrate yield similar to secondary RO<sub>2</sub> from MVK.<sup>18</sup> <sup>P</sup> Products for C2CO<sub>2</sub> are not included in the kinetic mechanism. <sup>Q</sup> Reactions replaced old reactions in base case of kinetic mechanism. See Table S5 for full names of the abbreviations used above.

**Table SA4.** List of photolysis reactions in the kinetic mechanism.

reaction	source of cross section	source of quantum yield	source of reaction
<b>basic reactions</b>			
H <sub>2</sub> O <sub>2</sub> + hv → 2OH	Kahan et al. <sup>67</sup>	JPL <sup>1</sup>	JPL <sup>1</sup>
O <sub>3</sub> + hv → O( <sup>1</sup> D) + O <sub>2</sub>	JPL <sup>1</sup>	JPL <sup>1</sup>	JPL <sup>1</sup>
O <sub>3</sub> + hv → O + O <sub>2</sub>	JPL <sup>1</sup>	JPL <sup>1</sup>	JPL <sup>1</sup>
NO <sub>2</sub> + hv → O + NO	JPL <sup>1</sup>	JPL <sup>1</sup>	JPL <sup>1</sup>
NO <sub>3</sub> + hv → NO + O <sub>2</sub>	JPL <sup>1</sup>	JPL <sup>1</sup>	JPL <sup>1</sup>
NO <sub>3</sub> + hv → NO <sub>2</sub> + O	JPL <sup>1</sup>	JPL <sup>1</sup>	JPL <sup>1</sup>
HONO + hv → OH + NO	JPL <sup>1</sup>	JPL <sup>1</sup>	JPL <sup>1</sup>
HNO <sub>3</sub> + hv → OH + NO <sub>2</sub>	JPL <sup>1</sup>	JPL <sup>1</sup>	JPL <sup>1</sup>
N <sub>2</sub> O <sub>5</sub> + hv → NO <sub>2</sub> + NO <sub>3</sub>	JPL <sup>1</sup>	JPL <sup>1</sup>	JPL <sup>1</sup>
<b>non-nitrate hydrocarbon reactions</b>			
CH <sub>2</sub> O + hv → 2HO <sub>2</sub> + CO	JPL <sup>1</sup>	JPL <sup>1</sup>	JPL <sup>1</sup>
CH <sub>2</sub> O + hv → H <sub>2</sub> + CO	JPL <sup>1</sup>	JPL <sup>1</sup>	JPL <sup>1</sup>
GLYC + hv → 2HO <sub>2</sub> + CO + CH <sub>2</sub> O	JPL <sup>1</sup>	JPL <sup>1</sup>	JPL <sup>1</sup>
GLYC + hv → CH <sub>3</sub> OH + CO	JPL <sup>1</sup>	JPL <sup>1</sup>	JPL <sup>1</sup>
GLYC + hv → OH + CH <sub>2</sub> CHO	JPL <sup>1</sup>	JPL <sup>1</sup>	JPL <sup>1</sup>



**Table SA4.** List of photolysis reactions in the kinetic mechanism.

reaction	source of cross section	source of quantum yield	source of reaction
HPETHNL + hv → Products	assume similar to GLYC	assume similar to GLYC	assume similar to GLYC
GLYX + hv → 2HO <sub>2</sub> + 2CO	JPL <sup>1</sup>	JPL <sup>1</sup>	JPL <sup>1</sup>
GLYX + hv → H <sub>2</sub> + 2CO	JPL <sup>1</sup>	JPL <sup>1</sup>	JPL <sup>1</sup>
GLYX + hv → CH <sub>2</sub> O + CO	JPL <sup>1</sup>	JPL <sup>1</sup>	JPL <sup>1</sup>
MGLYX + hv → CH <sub>3</sub> CO + HO <sub>2</sub> + CO	JPL <sup>1</sup>	JPL <sup>1</sup>	JPL <sup>1</sup>
MACR + hv → CH <sub>2</sub> CCH <sub>3</sub> + HO <sub>2</sub> + CO	MCM v3.2 <sup>4</sup>	MCM v3.2 <sup>4</sup>	MCM v. 3.2 <sup>4</sup>
MACR + hv → CH <sub>2</sub> CCH <sub>3</sub> CO + HO <sub>2</sub>	MCM v3.2 <sup>4</sup>	MCM v3.2 <sup>4</sup>	MCM v. 3.2 <sup>4</sup>
MVK + hv → CH <sub>3</sub> CHCH <sub>2</sub> + CO	MCM v3.2 <sup>4</sup>	MCM v3.2 <sup>4</sup>	MCM v. 3.2 <sup>4</sup>
MVK + hv → CH <sub>3</sub> CO + CH <sub>2</sub> CH	MCM v3.2 <sup>4</sup>	MCM v3.2 <sup>4</sup>	MCM v. 3.2 <sup>4</sup>
ISOPOOH + hv → IHO + OH	MCM v3.2 <sup>4</sup>	MCM v3.2 <sup>4</sup>	MCM v. 3.2 <sup>4</sup>
<b>nitrate hydrocarbon reactions</b>			
CH <sub>3</sub> ONO + hv → NO + HO <sub>2</sub> + CH <sub>2</sub> O	JPL <sup>1</sup>	JPL <sup>1</sup>	JPL <sup>1</sup>
INP + hv → INO + OH	MCM v3.2 <sup>4</sup>	MCM v3.2 <sup>4</sup>	MCM v. 3.2 <sup>4</sup>
IHPN + hv → IHNO + OH	assume same as INP	assume same as INP	assume same as INP
ICN + hv → PROPNN + 2CO + 2HO <sub>2</sub>	MCM v3.2 <sup>4</sup>	0.00195, MCM v3.2 <sup>4</sup>	MCM v. 3.2 <sup>4</sup>
IHN + hv → IO + NO <sub>2</sub>	MCM v3.2 <sup>4</sup>	MCM v3.2 <sup>4</sup>	MCM v. 3.2 <sup>4</sup>
IHCN + hv → NO <sub>2</sub> + Products	assume same as MVK	assume same as MVK	assume O-NO <sub>2</sub> breaks
IDHN + hv → NO <sub>2</sub> + Products	assume same as IHN	assume same as IHN	assume same as IHN
C4DCN + hv → NO <sub>2</sub> + Products	assume same as MGLYX	assume same as MGLYX	assume O-NO <sub>2</sub> breaks
C4CHN_A + hv → NO <sub>2</sub> + Products	assume same as C <sub>3</sub> H <sub>7</sub> CHO <sup>A</sup>	assume same as C <sub>3</sub> H <sub>7</sub> CHO	assume O-NO <sub>2</sub> breaks
C4CPN_A + hv → OH + MGLYX + CH <sub>2</sub> O + NO <sub>2</sub>	assume same as INP	assume same as INP	assume same as INP
C4CHN_K + hv → NO <sub>2</sub> + Products	assume same as MEK <sup>B</sup>	assume same as MEK	assume O-NO <sub>2</sub> breaks
C4CPN_K + hv → OH + MGLYX + CH <sub>2</sub> O + NO <sub>2</sub>	assume same as INP	assume same as INP	assume same as INP
PROPNN + hv → CH <sub>3</sub> COCH <sub>2</sub> O + NO <sub>2</sub>	MCM v3.2 <sup>4</sup>	MCM v3.2 <sup>4</sup>	MCM v3.2 <sup>4</sup>
PROPNN + hv → CH <sub>3</sub> CO + CH <sub>2</sub> O + NO <sub>2</sub>	MCM v3.2 <sup>4</sup>	MCM v3.2 <sup>4</sup>	MCM v3.2 <sup>4</sup>
ETHLN + hv → CH <sub>2</sub> O + CO + HO <sub>2</sub> + NO <sub>2</sub>	MCM v3.2 <sup>4</sup>	MCM v3.2 <sup>4</sup>	MCM v3.2 <sup>4</sup>
ETHLN + hv → CH <sub>2</sub> O + CO + HO <sub>2</sub> + NO <sub>2</sub>	MCM v3.2 <sup>4</sup>	MCM v3.2 <sup>4</sup>	MCM v3.2 <sup>4</sup>
<b>revised photolysis reactions (Section 4.4.2)</b>			
ICN + hv → PROPNN + 2CO + 2HO <sub>2</sub> *	assume same as MACR	1, Muller et al. <sup>68</sup>	MCM v. 3.2 <sup>4</sup>
C4DCN + hv → NO <sub>2</sub> + Products *	assume same as MGLYX	1, Muller et al. <sup>68</sup>	assume O-NO <sub>2</sub> breaks
C4CPN_A + hv → OH + MGLYX + CH <sub>2</sub> O + NO <sub>2</sub>	assume same as C <sub>3</sub> H <sub>7</sub> CHO	1, Muller et al. <sup>68</sup> , Wolfe et al. <sup>69</sup>	assume same as INP
C4CPN_K + hv → OH + MGLYX + CH <sub>2</sub> O + NO <sub>2</sub>	assume same as MEK	1, Muller et al. <sup>68</sup> , Wolfe et al. <sup>69</sup>	assume same as INP

**Table SA4.** List of photolysis reactions in the kinetic mechanism.

reaction	source of cross section	source of quantum yield	source of reaction
PROPNN + hv → CH <sub>3</sub> COCH <sub>2</sub> O + NO <sub>2</sub> *	MCM v3.2 <sup>4</sup>	Muller et al. <sup>68</sup>	MCM v. 3.2 <sup>4</sup>
PROPNN + hv → CH <sub>3</sub> CO + CH <sub>2</sub> O + NO <sub>2</sub> *	MCM v3.2 <sup>4</sup>	Muller et al. <sup>68</sup>	MCM v. 3.2 <sup>4</sup>
ETHLN + hv → CH <sub>2</sub> O + CO + HO <sub>2</sub> + NO <sub>2</sub> *	MCM v3.2 <sup>4</sup>	Muller et al. <sup>68</sup>	MCM v. 3.2 <sup>4</sup>
ETHLN + hv → CH <sub>2</sub> O + CO + HO <sub>2</sub> + NO <sub>2</sub> *	MCM v3.2 <sup>4</sup>	Muller et al. <sup>68</sup>	MCM v. 3.2 <sup>4</sup>

Notes: See Table S5 for full names of the abbreviations used above. \* Reactions replaced old reactions in kinetic mechanism. <sup>A</sup> In MCM v3.2<sup>4</sup> MACRNO<sub>3</sub> photolysis is also based on C<sub>3</sub>H<sub>7</sub>CHO. <sup>B</sup> Backbone structure is similar to MEK so like MCM v3.2<sup>4</sup> does for functionalized nitrates assumed this compound photolyzed like MEK.

**Table SA5.** Full name of abbreviations used in the kinetic mechanism.

abbreviation	name
C2CO <sub>2</sub>	ethanal peroxy radical
C3CHO <sub>2</sub>	hydroxy acetone peroxy radical
C3CNO <sub>2</sub>	propanone nitrate peroxy radical
C3CPO <sub>2</sub>	hydroperoxy acetone peroxy radical
C3DCO <sub>2</sub>	methyl glyoxal peroxy radical
C <sub>3</sub> H <sub>7</sub> CHO	2-methylpropanal
C4CHN	C <sub>4</sub> carbonyl hydroxynitrate
C4CHP	C <sub>4</sub> carbonyl hydroxy hydroperoxide
C4CN	C <sub>4</sub> carbonyl nitrate with one double bond
C4CPN	C <sub>4</sub> nitrooxycarbonyl hydroperoxide
C4DCH	C <sub>4</sub> hydroxy dicarbonyl
C4DCN	C <sub>4</sub> dicarbonyl nitrate
CH <sub>2</sub> (OH) <sub>2</sub>	methanediol
CH <sub>2</sub> CCH <sub>3</sub>	CH <sub>2</sub> C <sup>•</sup> CH <sub>3</sub>
CH <sub>2</sub> CCH <sub>3</sub> CO	CH <sub>2</sub> CCH <sub>3</sub> C <sup>•</sup> O
CH <sub>2</sub> CH	CH <sub>2</sub> C <sup>•</sup> H
CH <sub>2</sub> CHO	C <sup>•</sup> H <sub>2</sub> CHO
CH <sub>2</sub> O	formaldehyde
CH <sub>3</sub> CHCH <sub>2</sub>	CH <sub>3</sub> CHCH <sub>2</sub>
CH <sub>3</sub> CO	CH <sub>3</sub> C <sup>•</sup> O
CH <sub>3</sub> OH	methanol
CO	carbon monoxide
CO <sub>2</sub>	carbon dioxide
ETHLN	ethanal nitrate
GLYC	glycolaldehyde
GLYX	glyoxal
H <sub>2</sub>	dihydrogen
H <sub>2</sub> O	water
H <sub>2</sub> O <sub>2</sub>	hydrogen peroxide
HACET	hydroxyacetone
HCOOH	formic acid
HMHP	hydroxymethyl hydroperoxide
HMP	hydroxymethyl peroxy radical (HOCH <sub>2</sub> O <sub>2</sub> )
HNO <sub>3</sub>	nitric acid
HO <sub>2</sub>	hydroperoxyl radical
HO <sub>2</sub> NO <sub>2</sub>	peroxynitric acid
HONO	nitrous acid
HOONO	peroxynitrous acid
HPAC	hydroperoxy acetone

**Table SA5.** Full name of abbreviations used in the kinetic mechanism.

abbreviation	name
HPETHNL	hydroperoxyethanal (not peracetic acid)
ICHE	C <sub>5</sub> carbonyl hydroxy epoxide
ICHNO <sub>2</sub> I4	C <sub>5</sub> carbonyl hydroxy nitrooxyperoxy radical (Capable of 1,4 H shift)
ICHNO <sub>2</sub> I5	C <sub>5</sub> carbonyl hydroxy nitrooxyperoxy radical (Capable of 1,5 H shift)
ICHPN	C <sub>5</sub> carbonyl hydroxy nitrooxy hydroperoxide
ICN	C <sub>5</sub> carbonyl nitrate
ICPDNAH	C <sub>5</sub> dinitrooxy peroxyacid hydroxide
ICPN	C <sub>5</sub> carbonylhydroperoxide nitrate
IDH	C <sub>5</sub> dihydroxy
IDHDN	C <sub>5</sub> dinitrate from IDHNO <sub>2</sub> δ/ IDHNO <sub>2</sub> β + NO
IDHN	C <sub>5</sub> dihydroxy nitrate
IDHNO <sub>2</sub> β	C <sub>5</sub> dihydroxy nitrooxyperoxy radical– β isomer
IDHNO <sub>2</sub> δ	C <sub>5</sub> dihydroxy nitrooxyperoxy radical – δ isomer
IDHPN	C <sub>5</sub> dihydroxy nitrooxy hydroperoxide
IDN	C <sub>5</sub> dinitrate
IDNE	C <sub>5</sub> dinitrooxy epoxide
IDPN	C <sub>5</sub> dihydroperoxide nitrate
IEPOX	C <sub>5</sub> hydroxy epoxide
IHC	C <sub>5</sub> hydroxy carbonyl
IHCDN	C <sub>5</sub> dinitrate from ICHNO <sub>2</sub> I4 + NO
IHCN	C <sub>5</sub> hydroxy carbonyl nitrate
IHDPN	C <sub>5</sub> hydroxy nitrooxy dihydroperoxide
IHNO	C <sub>5</sub> hydroxy nitrooxyalkoxy radical
IHNO <sub>2</sub>	C <sub>5</sub> hydroxy nitrooxyperoxy radical (1,5 H shift product)
IHNO <sub>2</sub> HM	ROOR product from IHNO <sub>2</sub> and HMP
IHNβ	C <sub>5</sub> hydroxy nitrate – β isomer
IHNδ	C <sub>5</sub> hydroxy nitrate – δ isomer
IHO	C <sub>5</sub> hydroxy alkoxy radical
IHO2	C <sub>5</sub> hydroxy peroxy radical
IHPDN	C <sub>5</sub> dinitrate from INPHO <sub>2</sub> β/INPHO <sub>2</sub> δ + NO
IHPE	C <sub>5</sub> hydroxy hydroperoxy epoxide
IHPN	C <sub>5</sub> hydroxy hydroperoxide nitrate
IN	C <sub>5</sub> nitrooxy radical
INCE	C <sub>5</sub> nitrooxy carbonyl epoxide
INHEβ	C <sub>5</sub> nitrooxy hydroxy epoxide – β isomer
INHEδ	C <sub>5</sub> nitrooxy hydroxy epoxide – δ isomer
INHEδ2	C <sub>5</sub> nitrooxy hydroxyl epoxide from NO <sub>3</sub> oxidation of IHN
INO	C <sub>5</sub> nitrooxyalkoxy radical
INO <sub>2</sub>	C <sub>5</sub> nitrooxyperoxy radical
INO <sub>2</sub> HM	ROOR product from INO <sub>2</sub> and HMP
INO <sub>2</sub> IHN	ROOR product from INO <sub>2</sub> and IHNO <sub>2</sub>
INO <sub>2</sub> IN	ROOR product from INO <sub>2</sub> and INO <sub>2</sub>
INO <sub>2</sub> N	C <sub>5</sub> nitrooxy nitrite
INO <sub>3</sub> N	C <sub>5</sub> dinitrate
INO <sub>4</sub> N	C <sub>5</sub> nitrooxy peroxy nitrate
INPE	C <sub>5</sub> nitrooxy hydroperoxy epoxide
INPHO <sub>2</sub> β	C <sub>5</sub> nitrooxy hydroperoxy hydroxy peroxy radical (From β isomers)
INPHO <sub>2</sub> δ	C <sub>5</sub> nitrooxy hydroperoxy hydroxy peroxy radical (From δ isomers)
INPβ	C <sub>5</sub> nitrooxy hydroperoxide – β isomer
INPδ	C <sub>5</sub> nitrooxy hydroperoxide – δ isomer
IPNO	C <sub>5</sub> hydroperoxide nitrooxyalkoxy radical
IPNO <sub>2</sub>	C <sub>5</sub> hydroperoxide nitrooxyperoxy radical

**Table SA5.** Full name of abbreviations used in the kinetic mechanism.

abbreviation	name
ISOP	isoprene
ISOPN	C <sub>5</sub> hydroxynitrate from OH oxidation chemistry
ISOPOOH	C <sub>5</sub> hydroxy hydroperoxide
MAA	methacrylic acid
MACR	methacrolein
MACRHO <sub>2</sub>	peroxy radical from OH addition to MACR
MACRO <sub>2</sub>	peroxy radical from H-abstraction of MACR
MGLYX	methylglyoxal
MHP	methyl hydroperoxide
MPAA	methacrylicperoxy acid
MVK	methyl vinyl ketone
MVKHO <sub>2</sub>	peroxy radical from OH addition to MVK
N <sub>2</sub> O <sub>5</sub>	dinitrogen pentoxide
NO	nitrogen monoxide
NO <sub>2</sub>	nitrogen dioxide
NO <sub>3</sub>	nitrate Radical
O	oxygen radical ( <sup>3</sup> P state)
O( <sup>1</sup> D)	oxygen radical ( <sup>1</sup> D state)
O <sub>2</sub>	molecular oxygen
O <sub>3</sub>	ozone
OH	hydroxyl radical
PENYLO <sub>2</sub>	propenyl peroxy radical
PROPNN	propanone nitrate

## REFERENCES

1. Sander, S. P.; Abbatt, J.; Barker, J. R.; Burkholder, J. B.; Friedl, R. R.; Golden, D. M.; Huie, R. E.; Kolb, C. E.; Kurylo, M. J.; Moortgat, G. K., et al. *Chemical Kinetics and Photochemical Data for Use in Atmospheric Studies, Evaluation No. 17*. JPL Publication 10-6: Jet Propulsion Laboratory, Pasadena, 2011.
2. Atkinson, R.; Baulch, D. L.; Cox, R. A.; Crowley, J. N.; Hampson, R. F.; Hynes, R. G.; Jenkin, M. E.; Rossi, M. J.; Troe, J.; Subcommittee, I. Evaluated Kinetic and Photochemical Data for Atmospheric Chemistry: Volume II – Gas Phase Reactions of Organic Species *Atmos. Chem. Phys.* **2006**, *6*, 3625-4055.
3. Atkinson, R.; Baulch, D. L.; Cox, R. A.; Crowley, J. N.; Hampson, R. F.; Hynes, R. G.; Jenkin, M. E.; Rossi, M. J.; Troe, J. Evaluated Kinetic and Photochemical Data for Atmospheric Chemistry: Volume I - Gas Phase Reactions of O<sub>x</sub>, HO<sub>x</sub>, NO<sub>x</sub> and SO<sub>x</sub> Species. *Atmos. Chem. Phys.* **2004**, *4*, 1461-1738.
4. Saunders, S. M.; Jenkin, M. E.; Derwent, R. G.; Pilling, M. J. Protocol for the Development of the Master Chemical Mechanism, MCMv3 (Part A): Tropospheric Degradation of Non-Aromatic Volatile Organic Compounds. *Atmos. Chem. Phys.* **2003**, *3*, 161-180.
5. Cantrell, C. A.; Stockwell, W. R.; Anderson, L. G.; Busarow, K. L.; Perner, D.; Schmeltekopf, A.; Calvert, J. G.; Johnston, H. S. Kinetic Study of the NO<sub>3</sub>-CH<sub>2</sub>O Reaction and Its Possible Role in Nighttime Tropospheric Chemistry. *J. Phys. Chem.* **1985**, *89*, 139-146.
6. Lee, L.; Teng, A. P.; Wennberg, P. O.; Crounse, J. D.; Cohen, R. C. On Rates and Mechanisms of OH and O<sub>3</sub> Reactions with Isoprene-Derived Hydroxy Nitrates. *J. Phys. Chem. A.* **2014**, *118*, 1622-1637.

7. Kwan, A. J.; Chan, A. W. H.; Ng, N. L.; Kjaergaard, H. G.; Seinfeld, J. H.; Wennberg, P. O. Peroxy Radical Chemistry and OH Radical Production during the NO<sub>3</sub>-Initiated Oxidation of Isoprene. *Atmos. Chem. Phys.* **2012**, *12*, 7499-7515.
8. Zabel, F.; Sahetchian, K. A.; Chachaty, C. ESR Spectra of Free Radicals Formed During the Gas-Phase Photo-Oxidation of Formaldehyde: Thermal Stability of the HOCH<sub>2</sub>OO Radical. *Chem. Phys. Lett.* **1987**, *134*, 433-437.
9. St. Clair, J. M.; Rivera-Rios, J. C.; Crounse, J. D.; Knap, H. C.; Bates, K. H.; Teng, A. P.; Jorgensen, S.; Kjaergaard, H. G.; Keutsch, F. N.; Wennberg, P. O. Kinetics and Products of the Reaction of the First-Generation Isoprene Hydroxy Hydroperoxide (ISOPOOH) with OH, in Review. *J. Phys. Chem. A* **2015**.
10. Kwok, E. S. C.; Atkinson, R. Estimation of Hydroxyl Radical Reaction Rate Constants for Gas-Phase Organic Compounds Using a Structure-Reactivity Relationship: An Update. *Atmos. Environ.* **1995**, *29*, 1685-1695.
11. Lockwood, A. L.; Shepson, P. B.; Fiddler, M. N.; Alaghmand, M. Isoprene Nitrates: Preparation, Separation, Identification, Yields, and Atmospheric Chemistry. *Atmos. Chem. Phys.* **2010**, *10*, 6169-6178.
12. Zhang, X.; Schwantes, R. H.; McVay, R. C.; Lignell, H.; Coggon, M. M.; Flagan, R. C.; Seinfeld, J. H. Vapor Wall Deposition in Teflon Chambers. *Atmos. Chem. Phys.* **2015**, *15*, 4197-4214.
13. Rollins, A. W.; Kiendler-Scharr, A.; Fry, J. L.; Brauers, T.; Brown, S. S.; Dorn, H.; Dube, W. P.; Fuchs, H.; Mensah, A.; Mentel, T. F., et al. Isoprene Oxidation by Nitrate Radical: Alkyl Nitrate and Secondary Organic Aerosol Yields. *Atmos. Chem. Phys.* **2009**, *9*, 6685-6703.
14. Kerdouci, J.; Picquet-Varrault, B.; Durand-Jolibois, R.; Gaimoz, C.; Doussin, J. F. An Experimental Study of the Gas-Phase Reactions of NO<sub>3</sub> Radicals with a Series of Unsaturated Aldehydes: *trans*-2-Hexenal, *trans*-2-Heptenal, and *trans*-2-Octenal. *J. Phys. Chem. A* **2012**, *116*, 10135-10142.
15. Jacobs, M. I.; Burke, W. J.; Elrod, M. J. Kinetics of the Reactions of Isoprene-Derived Hydroxynitrates: Gas Phase Epoxide Formation and Solution Phase Hydrolysis. *Atmos. Chem. Phys.* **2014**, *14*, 8933-8946.
16. Lee, L. Interactive Comment on "Kinetics of the Reactions of Isoprene-Derived Hydroxynitrates: Gas Phase Epoxide Formation and Solution Phase Hydrolysis" by M. I. Jacobs et al. *Atmos. Chem. Phys. Discuss.* **2014**, *14*, C3249-C3251.
17. Teng, A. P.; Crounse, J. D.; Lee, L.; St. Clair, J. M.; Cohen, R. C.; Wennberg, P. O. Hydroxy Nitrate Production in the OH-Initiated Oxidation of Alkenes. *Atmos. Chem. Phys.* **2015**, *15*, 4297-4316.
18. Praske, E.; Crounse, J. D.; Bates, K. H.; Kurten, T.; Kjaergaard, H. G.; Wennberg, P. O. Atmospheric Fate of Methyl Vinyl Ketone: Peroxy Radical Reactions with NO and HO<sub>2</sub>. *J. Phys. Chem. A* **2015**, *119*, 4562-4572.
19. Crounse, J. D.; Knap, H. C.; Ørnsø, K. B.; Jørgensen, S.; Paulot, F.; Kjaergaard, H. G.; Wennberg, P. O. Atmospheric Fate of Methacrolein. 1. Peroxy Radical Isomerization Following Addition of OH and O<sub>2</sub>. *J. Phys. Chem. A* **2012**, *116*, 5756-5762.
20. Crounse, J. D.; Paulot, F.; Kjaergaard, H. G.; Wennberg, P. O. Peroxy Radical Isomerization in the Oxidation of Isoprene. *Phys. Chem. Chem. Phys.* **2011**, *13*, 13607-13613.
21. Crounse, J. D.; Nielsen, L. B.; Jørgensen, S.; Kjaergaard, H. G.; Wennberg, P. O. Autoxidation of Organic Compounds in the Atmosphere. *J. Phys. Chem. Lett.* **2013**, *4*, 3513-3520.

22. Carter, W. P. L.; Atkinson, R. Atmospheric Chemistry of Alkanes. *J. Atmos. Chem.* **1985**, *3*, 377-405.
23. Grosjean, E.; de Andrade, J. B.; Grosjean, D. Carbonyl Products of the Gas-Phase Reaction of Ozone with Simple Alkenes. *Environ. Sci. Technol.* **1996**, *30*, 983.
24. Tuazon, E. C.; Aschmann, S. M.; Arey, J.; Atkinson, R. Products of the Gas-Phase Reactions of O<sub>3</sub> with a Series of Methyl-Substituted Ethenes. *Environ. Sci. Technol.* **1997**, *31*, 3004-3009.
25. Taatjes, C. A.; Welz, O.; Eskola, A. J.; Savee, J. D.; Osborn, D. L.; Lee, E. P. F.; Dyke, J. M.; Mok, D. W. K.; Shallcross, D. E.; Percival, C. J. Direct Measurement of Criegee Intermediate (CH<sub>2</sub>OO) Reactions with Acetone, Acetaldehyde, and Hexafluoroacetone. *Phys. Chem. Chem. Phys.* **2012**, *14*, 10391-10400.
26. Rollins, A. W.; Browne, E. C.; Min, K. E.; Pusede, S. E.; Wooldridge, P. J.; Gentner, D. R.; Goldstein, a. H.; Liu, S.; Day, D. a.; Russell, L. M., et al. Evidence for NO<sub>x</sub> Control over Nighttime SOA Formation. *Science* **2012**, *337*, 1210-1212.
27. Bates, K. H.; Crounse, J. D.; St. Clair, J. M.; Bennett, N. B.; Nguyen, T. B.; Seinfeld, J. H.; Stoltz, B. M.; Wennberg, P. O. Gas Phase Production and Loss of Isoprene Epoxydiols. *J. Phys. Chem. A* **2014**, *118*, 1237-1246.
28. Jacobs, M. I.; Darer, A. I.; Elrod, M. J. Rate Constants and Products of the OH Reaction with Isoprene-Derived Epoxides. *Environ. Sci. Technol.* **2013**, *47*, 12868-12876.
29. Nguyen, T. B.; Crounse, J. D.; Schwantes, R. H.; Teng, A. P.; Bates, K. H.; Zhang, X.; St. Clair, J. M.; Brune, W. H.; Tyndall, G. S.; Keutsch, F. N., et al. Overview of the Focused Isoprene eXperiment at the California Institute of Technology (FIXCIT): Mechanistic Chamber Studies on the Oxidation of Biogenic Compounds. *Atmos. Chem. Phys.* **2014**, *14*, 13531-13549.
30. Jenkin, M. E.; Boyd, A. A.; Lesclaux, R. Peroxy Radical Kinetics Resulting from the OH-Initiated Oxidation of 1, 3-Butadiene, 2, 3-Dimethyl-1, 3-Butadiene and Isoprene. *J. Atmos. Chem.* **1998**, *29*, 267-298.
31. Skov, H.; Hjorth, J.; Lohse, C.; Jensen, N. R.; Restelli, G. Products and Mechanisms of the Reactions of the Nitrate Radical (NO<sub>3</sub>) with Isoprene, 1,3-Butadiene and 2,3-Dimethyl-1,3-Butadiene in Air. *Atmos. Environ.* **1992**, *26A*, 2771-2783.
32. Berndt, T.; Boge, O. Gas-Phase Reaction of NO<sub>3</sub> Radicals with Isoprene : A Kinetic and Mechanistic Study. *Int. J. Chem. Kinet.* **1997**, *29*, 755-765.
33. Suh, I.; Lei, W.; Zhang, R. Experimental and Theoretical Studies of Isoprene Reaction with NO<sub>3</sub>. *J. Phys. Chem. A* **2001**, *105*, 6471-6478.
34. Paulot, F.; Crounse, J. D.; Kjaergaard, H. G.; Kürten, A.; St. Clair, J. M.; Seinfeld, J. H.; Wennberg, P. O. Unexpected Epoxide Formation in the Gas-Phase Photooxidation of Isoprene. *Science* **2009**, *325*, 730-733.
35. Beaver, M. R.; St. Clair, J. M.; Paulot, F.; Spencer, K. M.; Crounse, J. D.; LaFranchi, B. W.; Min, K. E.; Pusede, S. E.; Wooldridge, P. J.; Schade, G. W., et al. Importance of Biogenic Precursors to the Budget of Organic Nitrates: Observations of Multifunctional Organic Nitrates by CIMS and TD-LIF during BEARPEX 2009. *Atmos. Chem. Phys.* **2012**, *12*, 5773-5785.
36. Ng, N. L.; Kwan, A. J.; Surratt, J. D.; Chan, A. W. H.; Chhabra, P. S.; Sorooshian, A.; Pye, H. O. T.; Crounse, J. D.; Wennberg, P. O.; Flagan, R. C., et al. Secondary Organic Aerosol (SOA) Formation from Reaction of Isoprene with Nitrate Radicals (NO<sub>3</sub>). *Atmos. Chem. Phys.* **2008**, *8*, 4117-4140.

37. Orlando, J. J.; Tyndall, G. S. Laboratory Studies of Organic Peroxy Radical Chemistry: An Overview with Emphasis on Recent Issues of Atmospheric Significance. *Chem. Soc. Rev.* **2012**, *41*, 6294-317.
38. Peeters, J.; Müller, J.-F.; Stavrou, T.; Nguyen, V. S. Hydroxyl Radical Recycling in Isoprene Oxidation Driven by Hydrogen Bonding and Hydrogen Tunneling: The Upgraded LIM1 Mechanism. *J. Phys. Chem. A* **2014**, *118*, 8625-8643.
39. Sprague, M. K.; Garland, E. R.; Mollner, A. K.; Bloss, C.; Bean, B. D.; Weichman, M. L.; Mertens, L. A.; Okumura, M. Kinetics of n-Butoxy and 2-Pentoxo Isomerization and Detection of Primary Products by Infrared Cavity Ringdown Spectroscopy. *J. Phys. Chem. A* **2012**, *116*, 6327-6340.
40. Xiong, J. Q.; Zhong, M.; Fang, C.; Chen, L. C.; Lippmann, M. Influence of Organic Films on the Hygroscopicity of Ultrafine Sulfuric Acid Aerosol. *Environ. Sci. Technol.* **1998**, *32*, 3536-3541.
41. Surratt, J. D.; Chan, a. W. H.; Eddingsaas, N. C.; Chan, M. N.; Loza, C. L.; Kwan, a. J.; Hersey, S. P.; Flagan, R. C.; Wennberg, P. O.; Seinfeld, J. H. Reactive Intermediates Revealed in Secondary Organic Aerosol Formation from Isoprene. *Proc. Natl. Acad. Sci. U. S. A.* **2010**, *107*, 6640-6645.
42. Lin, Y.-H.; Zhang, Z.; Docherty, K. S.; Zhang, H.; Budisulistiorini, S. H.; Rubitschun, C. L.; Shaw, S. L.; Knipping, E. M.; Edgerton, E. S.; Kleindienst, T. E., et al. Isoprene Epoxydiols as Precursors to Secondary Organic Aerosol Formation: Acid-Catalyzed Reactive Uptake Studies with Authentic Compounds. *Environ. Sci. Technol.* **2012**, *46*, 250-258.
43. Nguyen, T. B.; Coggon, M. M.; Bates, K. H.; Zhang, X.; Schwantes, R. H.; Schilling, K. A.; Loza, C. L.; Flagan, R. C.; Wennberg, P. O.; Seinfeld, J. H. Organic Aerosol Formation from the Reactive Uptake of Isoprene Epoxydiols (IEPOX) onto Non-Acidified Inorganic Seeds. *Atmos. Chem. Phys.* **2014**, *14*, 3497-3510.
44. Hu, W. W.; Campuzano-Jost, P.; Palm, B. B.; Day, D. A.; Ortega, A. M.; Hayes, P. L.; Krechmer, J. E.; Chen, Q.; Kuwata, M.; Liu, Y. J., et al. Characterization of a Real-Time Tracer for Isoprene Epoxydiols-Derived Secondary Organic Aerosol (IEPOX-SOA) from Aerosol Mass Spectrometer Measurements. *Atmos. Chem. Phys. Discuss.* **2015**, *15*, 11223-11276.
45. Darer, A. I.; Cole-Filipiak, N. C.; O'Connor, A. E.; Elrod, M. J. Formation and Stability of Atmospherically Relevant Isoprene-Derived Organosulfates and Organonitrates. *Environ. Sci. Technol.* **2011**, *45*, 1895-1902.
46. Hu, K. S.; Darer, A. I.; Elrod, M. J. Thermodynamics and Kinetics of the Hydrolysis of Atmospherically Relevant Organonitrates and Organosulfates. *Atmos. Chem. Phys.* **2011**, *11*, 8307-8320.
47. Surratt, J. D.; Kroll, J. H.; Kleindienst, T. E.; Edney, E. O.; Claeys, M.; Sorooshian, A.; Ng, N. L.; Offenberg, J. H.; Lewandowski, M.; Jaoui, M., et al. Evidence for Organosulfate in Secondary Organic Aerosol. *Environ. Sci. Technol.* **2007**, *41*, 517-527.
48. Gomez-Gonzalez, Y.; Surratt, J. D.; Cuyckens, F.; Szmigielski, R.; Vermeylen, R.; Jaoui, M.; Lewandowski, M.; Offenberg, J. H.; Kleindienst, T. E.; Edney, E. O., et al. Characterization of Organosulfates from the Photooxidation of Isoprene and Unsaturated Fatty Acids in Ambient Aerosol Using Liquid Chromatography/(-) Electrospray Ionization Mass Spectrometry. *J. Mass Spectrom.* **2008**, *43*, 371-382.
49. Hatch, L. E.; Creamean, J. M.; Ault, A. P.; Surratt, J. D.; Chan, M. N.; Seinfeld, J. H.; Edgerton, E. S.; Su, Y.; Prather, K. A. Measurements of Isoprene-Derived Organosulfates in

Ambient Aerosols by Aerosol Time-of-Flight Mass Spectrometry-Part 2: Temporal Variability and Formation Mechanisms. *Environ. Sci. Technol.* **2011**, *45*, 8648-8655.

50. Marklund, S. The Simultaneous Determination of Bis(hydroxymethyl)-Peroxide (BHMP), Hydroxymethylhydroperoxide (HMP), and  $\text{H}_2\text{O}_2$  with Titanium(IV). Equilibria Between the Peroxides and the Stabilities of HMP and BHMP at Physiological Conditions. *Acta Chem. Scand.* **1971**, *25*, 3517-3531.
51. Yadav, G. D.; Surve, P. S. Atom Economical Green Synthesis of Chloromethyl-1,3-dioxolanes from Epichlorohydrin Using Supported Heteropolyacids. *Ind. Eng. Chem. Res.* **2013**, *52*, 6129-6137.
52. Jenkin, M. E.; Hurley, M. D.; Wallington, T. J. Investigation of the Radical Product Channel of the  $\text{CH}_3\text{COO}_2 + \text{HO}_2$  Reaction in the Gas Phase. *Phys. Chem. Chem. Phys.* **2007**, *9*, 3149-3162.
53. Paulot, F.; Crounse, J. D.; Kjaergaard, H. G.; Kroll, J. H.; Seinfeld, J. H.; Wennberg, P. O. Isoprene Photooxidation: New Insights into the Production of Acids and Organic Nitrates. *Atmos. Chem. Phys.* **2009**, *9*, 1479-1501.
54. Jenkin, M. E.; Saunders, S. M.; Pilling, M. J. The Tropospheric Degradation of Volatile Organic Compounds: A Protocol for Mechanism Development. *Atmos. Environ.* **1997**, *31*, 81-104.
55. Liu, Y. J.; Herdinger-Blatt, I.; McKinney, K. A.; Martin, S. T. Production of Methyl Vinyl Ketone and Methacrolein via the Hydroperoxyl Pathway of Isoprene Oxidation. *Atmos. Chem. Phys.* **2013**, *13*, 5715-5730.
56. Bernard, F.; Cazaunau, M.; Mu, Y.; Wang, X.; Daele, V.; Chen, J.; Mellouki, A. Reaction of  $\text{NO}_2$  with Selected Conjugated Alkenes. *J. Phys. Chem. A* **2013**, *117*, 14132-14140.
57. Canosa, C.; Penzhorn, R. D.; Sonntag, C. V. Product Quantum Yields from the Photolysis of  $\text{NO}_2$  at 366 nm in the Presence of Ethylene. – The Role of  $\text{NO}_3^*$ . *Ber. Bunsenges. Phys. Chem.* **1979**, *83*, 217-225.
58. Orlando, J. J.; Tyndall, G. S.; Paulson, S. E. Mechanism of the OH-Initiated Oxidation of Methacrolein *Geophys. Res. Lett.* **1999**, *26*, 2191-2194.
59. Hasson, A. S.; Tyndall, G. S.; Orlando, J. J. A Product Yield Study of the Reaction of  $\text{HO}_2$  Radicals with Ethyl Peroxy ( $\text{C}_2\text{H}_5\text{O}_2$ ), Acetyl Peroxy ( $\text{CH}_3\text{C}(\text{O})\text{O}_2$ ), and Acetonyl Peroxy ( $\text{CH}_3\text{C}(\text{O})\text{CH}_2\text{O}_2$ ) Radicals. *J. Phys. Chem. A* **2004**, *108*, 5979-5989.
60. Hasson, A. S.; Tyndall, G. S.; Orlando, J. J.; Singh, S.; Hernandez, S. Q.; Campbell, S.; Ibarra, Y. Branching Ratios for the Reaction of Selected Carbonyl-Containing Peroxy Radicals with Hydroperoxy Radicals. *J. Phys. Chem. A* **2012**, *116*, 6264-6281.
61. Aschmann, S. M.; Atkinson, R. Formation Yields of Methyl Vinyl Ketone and Methacrolein from the Gas-Phase Reaction of  $\text{O}_3$  with Isoprene. *Environ. Sci. Technol.* **1994**, *28*, 1539-42.
62. Grosjean, D.; Williams, E. L.; Grosjean, E. Atmospheric Chemistry of Isoprene and Its Carbonyl Products. *Environ. Sci. Technol.* **1993**, *27*, 830-840.
63. Atkinson, R.; Aschmann, S. M.; Arey, J.; Shorees, B. Formation of OH Radicals in the Gas Phase Reactions of  $\text{O}_3$  with a Series of Terpenes. *J. Geophys. Res.* **1992**, *97 (D5)*, 6065-6073.
64. Paulson, S. E.; Flagan, R. C.; Seinfeld, J. H. Atmospheric Photooxidation of Isoprene Part II: The Ozone-Isoprene Reaction. *Int. J. Chem. Kinet.* **1992**, *24*, 103-125.



65. Neeb, P.; Moortgat, G. K. Formation of OH Radicals in the Gas-Phase Reaction of Propene, Isobutene, and Isoprene with O<sub>3</sub>: Yields and Mechanistic Implications. *J. Phys. Chem. A* **1999**, *103*, 9003-9012.
66. Malkin, T. L.; Goddard, A.; Heard, D. E.; Seakins, P. W. Measurements of OH and HO<sub>2</sub> Yields from the Gas Phase Ozonolysis of Isoprene. *Atmos. Chem. Phys.* **2010**, *10*, 1441-1459.
67. Kahan, T. F.; Washenfelder, R. a.; Vaida, V.; Brown, S. S. Cavity-Enhanced Measurements of Hydrogen Peroxide Absorption Cross Sections from 353 to 410 nm. *J. Phys. Chem. A* **2012**, *116*, 5941-5947.
68. Muller, J. F.; Peeters, J.; Stavrakou, T. Fast Photolysis of Carbonyl Nitrates from Isoprene. *Atmos. Chem. Phys.* **2014**, *14*, 2497-2508.
69. Wolfe, G. M.; Crounse, J. D.; Parrish, J. D.; St. Clair, J. M.; Beaver, M. R.; Paulot, F.; Yoon, T. P.; Wennberg, P. O.; Keutsch, F. N. Photolysis, OH Reactivity and Ozone Reactivity of a Proxy for Isoprene-Derived Hydroperoxyenals (HPALDs). *Phys. Chem. Chem. Phys.* **2012**, *14*, 7276-7286.